Influence of halloysite nanotubes onto the fire properties of polymer based composites

Euphrasie Jasinski, Véronique Bounor-Legaré, Aurélie Taguet, Emmanuel Beyou

Influence of halloysite nanotubes onto the fire properties of polymer based composites: A review

Euphrasie Jasinski[a], Véronique Bounor-Legaré[a], Aurélie Taguet[b], Emmanuel Beyou[a,*]

[a] Univ Lyon, Université Lyon1, CNRS UMR 5223, Ingénierie des Matériaux Polymères, Lyon, F-69621, France
[b] Polymers Composites and Hybrids (PCH), IMT Mines Ales, Ales, France

A B S T R A C T

Fire retardancy is of crucial importance for most of the polymer applications and fire proofing materials are often based on polymer blends with high fire retardants contents (up to 60wt%) which induce cost in- crease and lower mechanical performances. The use of ammonium polyphosphate (APP) as fire retardant allows maintaining good mechanical properties but it can be removed from the polymer matrix under hygrothermal conditions. In this context, halloysite nanotubes (HNTs) offer a good alternative as carriers of flame retardant systems to control the migration of the flame retardant molecules encapsulated in the HNT lumen for long-term aging properties. This review highlights the influence of the presence of HNTs and its derivatives on the fire retardancy performances of polymer-based composites. The discussion is examined according to the nature of the polymer from thermoplastics to thermosets.

Keywords:
Halloysite nanotubes
Flame retardancy
Thermoplastics
Thermosets
Elastomers

1. Introduction

Polymers are widely used in different fields such as packaging, building or electrical industries because of their good mechanical properties regarding their density. However, their poor fire retardant properties limit some of their applications [1]. In general, polymer combustion is based on a combination of an energy feedback from a flame to the polymer surface and the generation of combustible degradation products coming from polymer gasification [2]. Thus, to protect the polymer against fire, it is necessary to reduce the heat released during the polymer combustion below the one required to maintain combustion; hence it is necessary to reduce the amount of flammable volatiles emitted during the polymer combustion by modifying the pyrolysis process through the prevention of the condensed phase from the presence of oxygen or the decrease of the heat flow. Therefore, flame retardants (FRs) are incorporated into a polymer matrix as an initial comonomer, a post-reagent or an additive using a melting process. Fire retardancy can also be obtained through the coating of an intumescent layer containing flame retardants on the polymer surface [3,4].

The industrial market has a wide range of FRs such as halogen, phosphorus and nitrogen containing compounds and metal hydroxides. However, halogen-based flame retardants and particularly brominated FR can produce dangerous toxic substances such as hydrogen halides gas during burning and may release corrosive smoke. Thus, their use is going down in Europe and some are even forbidden [2,5]. Phosphorus containing compounds are a wide range of FR. Phosphines [6], phosphine oxides [7,8], phosphonates [9,10], elemental red phosphorus [11], phosphites [12] and phosphate [13] are all used as FRs in polymers. These compounds mostly act in the condensed phase by increasing the amount of carbonaceous char [14]. Nitrogen-based FRs have lower fire retardancy efficiency than halogen-based FRs but they are environmentally friendly because they release lower amount of smoke during burning [15]. Ammonium polyphosphate, melamine and its salts are the most used nitrogen-based FRs [2]. Moreover, metal hydroxides are one of the most used FRs because they are non-toxic and cheap but they must be used in high loading (>40 wt%) to obtain the desired flame retardancy leading to a detrimental impact on the mechanical properties and density in particular [16]. The flame retardancy of polymers can also be improved by the use of intumescent systems [17]. Intumescent formulations contain three ingredients: an acid source (e.g. phosphate, borate), a carbonization compound and a blowing agent (e.g. melamine, isocyanurate) [18]. During burning, they form a protective char layer on the polymer surface. More recently, some authors focused their attention on the use of nanomaterials to form nanocomposites with enhanced fire properties. It has been reported that the use of well dispersed nanofillers (kaolin [19], expanded graphite [20,21], carbon nanotubes [22], silicates such as montmorillonite [23] or halloysite nanotubes) in nanocomposites leads to an improvement of flame retardancy and thermal stability [24]. The combination of

* Corresponding author.
E-mail address: emmanuel.beyou@univ-lyon1.fr (E. Beyou).

Table 1
Characteristics of halloysites from different locations [31].

Halloysite trade name	Origin	Purity (%)	Length range (nm)*	Inner diameter range (nm)*	Outer diameter range (nm)*	Lumen space (vol%)	S_{BET} (m^2/g)
CLA	South Australia	95	100-1500	10-50	20-70	34	74.66
MB	New Zealand	87	100-3000	15-70	50-200	11	22.10
DG	North America	84	50-1500	5-30	20-150	26	57.30
TP	New Zealand	98	100-1500	10-20	30-50	19	33.31
PATCH	Western Australia	98	200-5000	12-22	40-55	39	81.59

* Results based on transmission electronic microscopy measurements for around 100 tubes from an average of 40 micrographs per sample

different FRs is often used to optimize the flame retardant performance of polymers [25]. For example, the use of 5 wt% layered silicate in combination with metal hydroxides such as aluminium trihydrate (ATH) in an EVA matrix allows the decrease of the total additives loading from 65 wt% down to 50 wt% while maintaining the same flame retardancy properties [26]. In addition, the use of halloysite nanotubes, coming from natural deposits and non-hazardous for the environment, is expected to limit the heat release and the mass transport. This review will thus deal with the main properties of the halloysite nanotubes that ensure better flame retardancy properties and it will be divided in four parts. In the first part, general informations about halloysite nanotubes are provided. The second part details the methods of incorporation of HNT into polymer matrices. Then, the different fire tests used to determine the fire retardancy of polymers are presented. Finally, the fire performances of halloysite nanotubes based nanocomposites are discussed according to the polymer matrix nature.

2. HNT: structure and properties

2.1. Generalities and structure

The name halloysite was first used in 1826 by Berthier and was derived from Omalius d'Halloy, who found the mineral in Belgium. The extensive research on halloysite began in the 1940s. Halloysite is a mineral of kaolinite group exhibiting a chemical composition based on $Al_2Si_2O_5(OH)_4.nH_2O$ where n equals 2 or 0. When n = 2, the HNT has a layer of water in the interlayer spaces. It is in a hydrated state and is called HNTs-10Å. When heating, it loses the water between the layers (n=0) and it changes irreversibly to HNTs-7Å [27]. HNT displays a hollow tubular structure with a high aspect ratio. Generally, HNTs have an inner diameter of 1-30 nm, an outer diameter of 30-50 nm and a length in the range 100-2000 nm (Fig. 1).

HNTs are inorganic nanotubes exhibiting a multi-walled structure and they have a 10.7–39vol% lumen space. Due to the empty lumen structures, the density of HNTs is relatively low (2.14–2.59 g/cm^3). The external surface is composed of siloxane (Si–O–Si) bonds with some silanol groups (Si–OH) and a few of aluminol groups (Al–OH) while both the interlayer and the internal lumen surfaces are composed of aluminol groups (Al–OH) [28]. It should be also mentioned that the inner and the outer surfaces of HNTs are positively and negatively charged, respectively. As HNTs are natural nanomaterials, their composition, sizes and properties are supplier dependent [29].

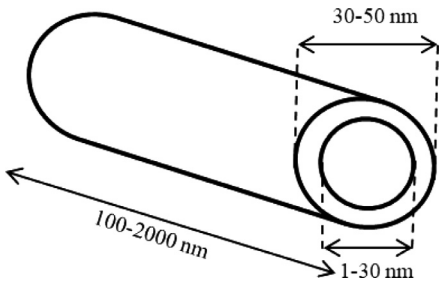

Fig. 1. Schematic representation of halloysite nanotubes.

2.2. Composition and characteristics of the main natural HNTs

HNTs are found naturally in rocks and soils in several countries such as Brazil, New Zealand, China, Korea, Japan, USA, Turkey, France, Belgium, etc [30]. Halloysites coming from different suppliers exhibit properties that depend on the country and the local conditions of formation [31]. Indeed, the origin of the HNTs has an influence on its chemical composition, size and surface area (Table 1).

CLA halloysite are uniform straight tubular particles which provide a good dispersibility in polymer matrices and they classically display a length range from 0.1 to 5 µm [31] but PATCH HNTs (Western Australia) have been also described with a length up to 30 µm [32]. In addition, some HNTs, such as CLA and TP, contain Fe_2O_3 as impurity, which may improve the thermal stability of their nanocomposites with polypropylene through a radical trapping [33]. In the following discussions, the sources of HNT will not be mentioned.

2.3. Applications and properties of HNTs

HNTs are used for different applications such as sorbents for pollutants [34], nanoreactors, nanofillers and for controlling the release of drugs [35]. Moreover, they are non-toxic and biocompatible [36]. They exhibit numerous applications in polymer nanocomposites because they have good properties such as a strong mechanical strength, a high thermal stability and a good availability [37]. Indeed, the incorporation of HNT into polymer nanocomposites improves their mechanical properties [38]. For example, Prashantha et al. [39] demonstrated that the addition of 6 wt% of HNT into PA6 increased the tensile modulus (from 2015 MPa to 2628 MPa) and the tensile strength (from 55 MPa to 72 MPa). The increase in Young modulus was also highlighted by incorporating 5 wt% of HNT in poly(hydroxybutyrate-co-hydroxyvalerate) (PHBV) with a Young modulus of 3.5 GPa for neat PHBV and 5.7 GPa for PHBV/5 wt% HNT [40]. In addition, by considering the thermal stability under nitrogen, it was shown that adding 10 phr of HNTs modified with an alkoxysilane into a PP matrix leads to a decomposition temperature of 60°C higher than the one of the PP matrix [41]. Moreover, HNTs influence polymers crystallization by acting as heterogeneous nucleating agents. For example, the addition of HNT in PLA resulted in notable improvement in PLA crystallinity with a crystallinity degree increase from 30% (neat PLA) to 47% (PLA/1 wt% HNT) [42]. In addition, the inclusion of HNT in epoxy matrix resulted in a significant reduction of the thermal expansion coefficient from 82.32 µm/(m.°C) (neat epoxy) to 68.68 µm/(m.°C) (epoxy/10 wt% HNT) [43]. HNTs are, as it will be deeply illustrated in this review, also used as environmentally friendly fire retardants in polymers because of their protection effect against heat

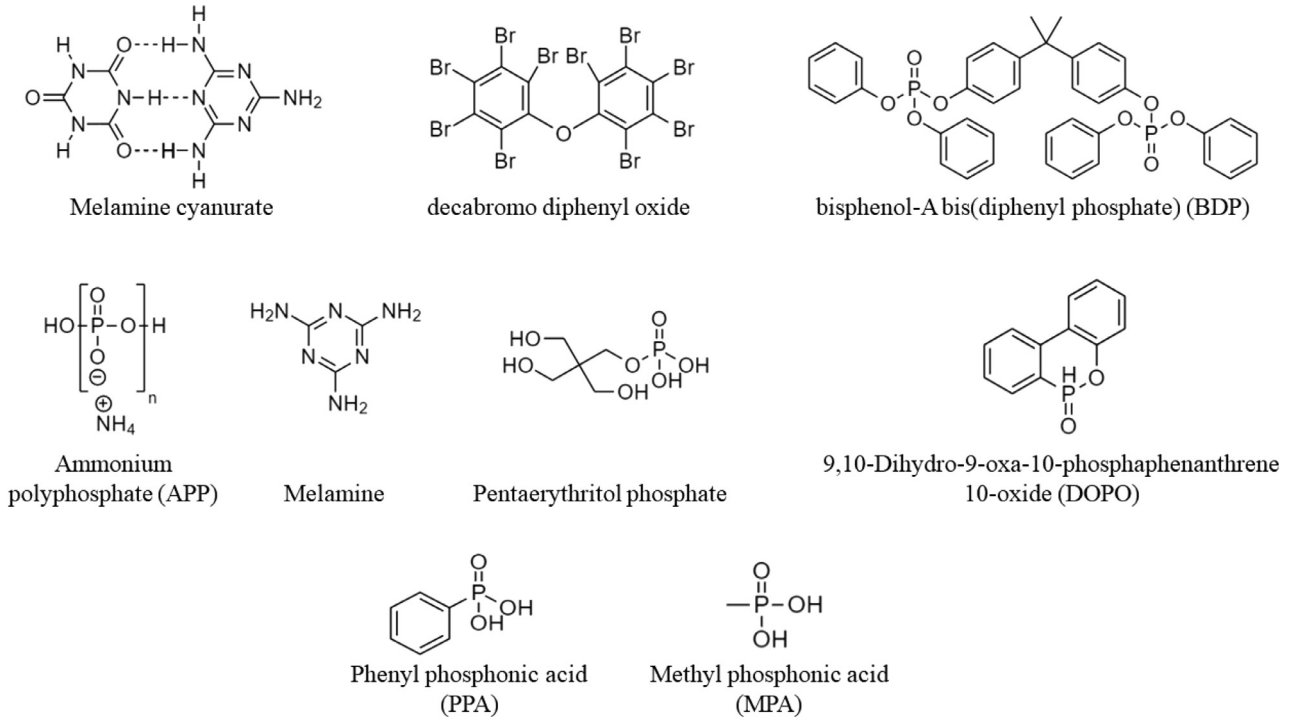

Fig. 2. Chemical structures of some flame retardants used in combination with HNT

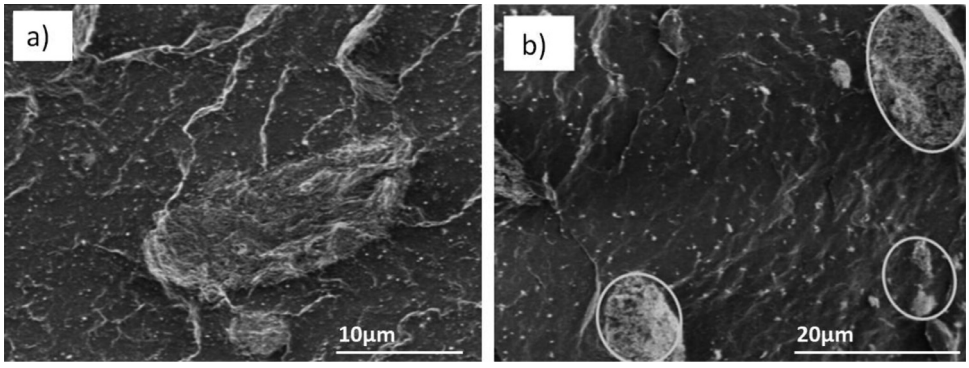

Fig. 3. (a) SEM image of 8 wt% HNTs dispersed in polyamide 12, PA12 (adapted from [50]), (b) SEM micrographs of 8 wt% HNTs dispersed in polypropylene, PP (adapted from [51]).

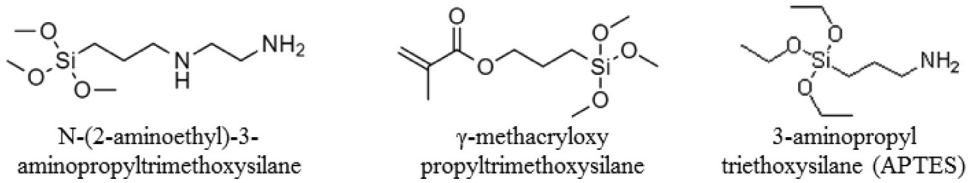

Fig. 4. Examples of molecules grafted onto HNT to improve its dispersion.

$$Al_2Si_5O_5(OH_4).2H_2O \xrightarrow[-2H_2O]{200°C} Al_2Si_5O_5(OH_4) \xrightarrow[-4OH]{600°C} Al_2Si_5O_5$$

Scheme 1. Thermal decomposition of halloysite nanotubes [44].

and mass transport during the burning of nanocomposites. Indeed, by increasing temperature, HNTs release adsorbed water molecules (T<200°C), followed by another weight loss (about 35wt%) at temperatures higher than 600°C that corresponds to the dehydroxylation of aluminol groups (Scheme 1) [44]. Finally, the formation of new solid phases is observed at temperatures higher than 880°C.

Thus, depending on the HNT concentration (up to 35wt%) in the nanocomposites and its surface treatment (for example, hydrophilic polysiloxanes), the release of water molecules may dilute combustible gases and inhibit the formation of toxic smokes. CO emission is due to a non-complete combustion during fire and the presence of HNT is expected to decrease the rate of the formation of toxic smokes [45]. Du et al. [35] proposed an entrapment mechanism of the decomposition products in the HNTs lumen to explain the enhancement of fire retardancy and thermal stability of the corresponding nanocomposites. In addition, the presence of iron-based molecules (between 0.30 wt% and 3.38 wt% of Fe_2O_3

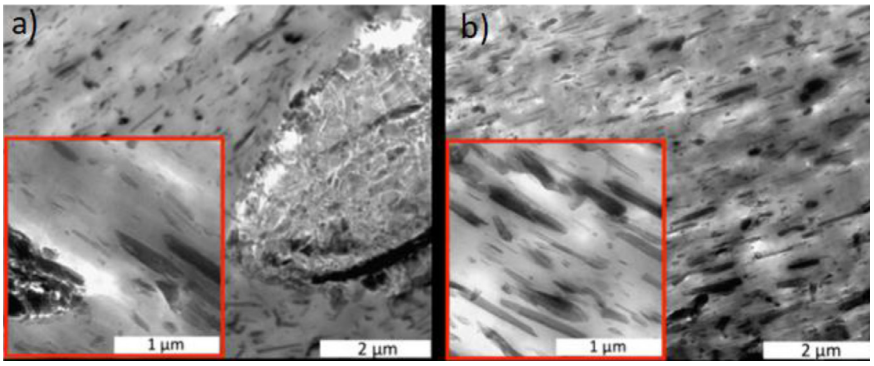

Fig. 5. TEM micrographs of (a) PA12/16wt%HNT and (b) PA12/16wt%HNT-W nanocomposites (reproduced with permission from [50],Copyright 2014, Wiley).

in HNTs [31]) can favor the decrease of the composite flammability as it was also observed for PP/carbon nanotubes [46] and PS/montmorillonite composites [47]. Actually, it was reported that iron oxides can trap the free radicals that usually propagate the fire reaction [48]. The pristine HNTs can also be incorporated in combination with other flame retardants (Fig. 2). These FR additives act in combination with HNTs to enhance the fire retardant properties of the nanocomposites and/or to reduce the total needed amount of FRs.

Moreover, to improve significantly the flame retardant property, it was shown that HNTs must be homogeneously dispersed in the polymer matrix [49]. Thus, HNTs dispersion is challenging in polar and apolar polymers [50,51] (Fig. 3).

3. Incorporation of HNTs in polymer matrices

To enhance their dispersion in polymer matrices, the HNTs can be incorporated through four different methods. The first method is the melt blending of HNTs and the polymer matrix by using the well-known melt compounding process, and more specifically the extrusion process. The incorporation of HNTs by using melt blending can also involve a pre-treatment through its surface modification with organic compounds (Fig. 4) or by a combination with compatibilizing agents in order to improve their dispersion.

Commonly used compatibilizers are polyolefins (PE or PP) grafted with maleic anhydride (MA), PE-g-MA and PP-g-MA respectively, which can ensure the formation of hydrogen bonds with the hydroxyl groups located onto the HNT surface [52].

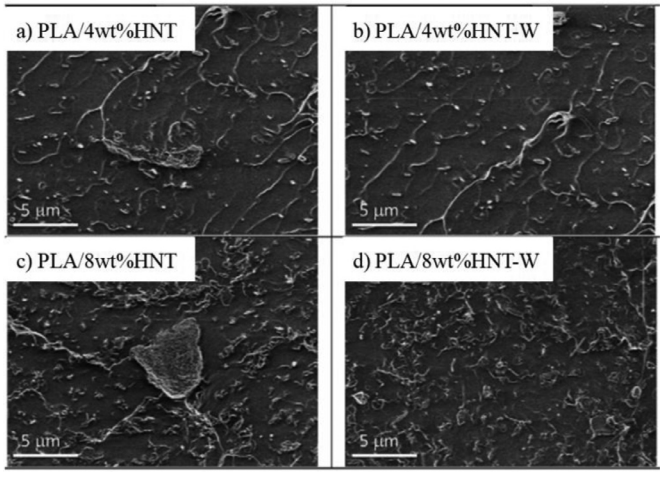

Fig. 6. SEM images of PLA nanocomposites (a) PLA/4wt%HNT, (b) PLA/4wt%HNT-W, (c) PLA/8wt%HNT, (d) PLA/8wt%HNT-W (adapted from [53]).

The extrusion process can also be combined with water injection. Indeed, the water-assisted extrusion process was used to improve the HNTs dispersion [51], as the dispersion state of the HNT may be a key factor to increase the fire retardant property of polymer composites. In the water-assisted extrusion, water is injected into a high compression zone of the extruder and then, degassed in a transport zone and completely removed using a vacuum pump. At high pressure and temperature, water remained liquid and miscibility with polymer depending on its nature could be achieved. Using this process, Lecouvet et al. [50] prepared PA12/HNT nanocomposites and they obtained an improved dispersion of HNT in the PA12 matrix especially for a HNTs content higher than 10 wt%. The water-assisted process lowered the viscosity of the blend which increased the mobility of the polymer chains and consequently their diffusion between the nanotubes. To illustrate this behaviour, the TEM images of the composites obtained by water-assisted extrusion showed a homogeneous dispersion of 16wt% HNT in PA12 (PA12/16wt%HNT-W, Fig. 5b) contrary to the composites obtained by a melt mixture of HNT and PA12 which exhibited some micron-sized aggregates of HNT (PA12/16wt%HNT, Fig. 5a).

Similarly to polyamide 12, the water-assisted extrusion process improved the dispersion of HNTs in polylactides (PLA) especially for HNTs contents higher than 8 wt% (Fig. 6) and in polyethersulfone (PES) [53].

Moreover, Lecouvet et al. [51,54] combined the water injection process with the use of a compatibilizer (PP-g-MA) to optimize the dispersion of the HNTs in PP. A masterbatch of PP, PP-g-MA (10 wt%) and HNTs (4 to 16 wt%) was prepared by water-assisted extrusion. The extrusion process was conducted at 200°C at a screw speed of 200 rpm while water was injected into the extruder with a 50 ml/min flow rate. The use of water injection to prepare a nanocomposite containing PP-g-MA and 8 wt% HNTs lead to well dispersed HNTs (nanosize) along with some micron size aggregates (Fig. 7d), while the melt blending of PP (or PP-g-MA) with HNT did not allow a good dispersion (lateral dimension of a few microns) (Fig. 7a and c, respectively).

The second method is the solution processing, where the nanotubes and the polymer are added in an appropriated solvent via vigorous stirring or ultrasonic bath. These solutions are then casted leading to a film or hydrogel [37]. For example, halloysite–polyvinyl alcohol (PVA) composite films were prepared by casting from aqueous solutions [55]. Nevertheless, the well-dispersed HNTs can re-agglomerate in the matrix during drying. The third method consists in the coating of a protective film containing HNTs onto the polymer surface instead of incorporated HNTs directly in the polymer matrix [56]. This method requires a smaller amount of HNTs and may lead to similar flame retardancy properties as the HNT-based nanocomposites without any coating layer. The fourth

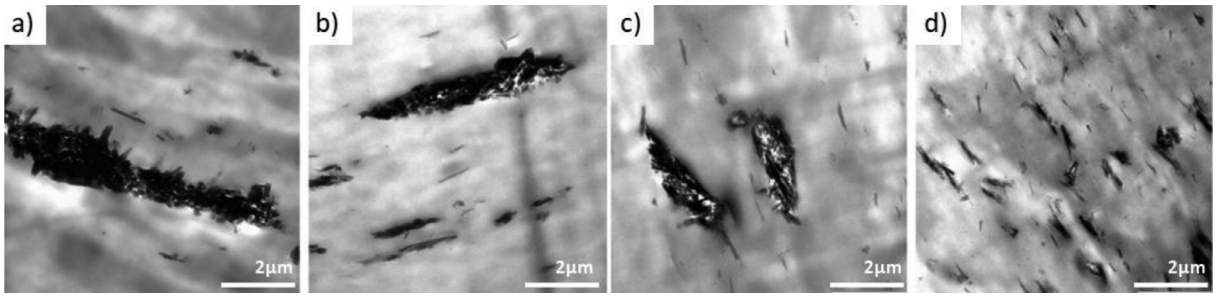

Fig. 7. TEM micrographs of: (a) PP/8wt%HNT, (b) PP/8wt%HNT-W, (c) PP/10wt%PP-g-MA/8wt%HNT and (d) PP/10wt%PP-g-MA/8wt%HNT-W nanocomposites (adapted from [51]).

method is based on the *in situ* polymerization approach. The HNTs are directly dispersed in a monomer, such as methyl methacrylate [57], which is further polymerized. The potential specific interaction between the monomer and the HNT can lead to a fine dispersion of the filler in the final polymer matrix [58].

Finally, whatever the method selected, the finer dispersion of HNT will allow enhancing properties and especially the flame retardancy of the nanocomposites. The mechanism of dispersion of HNTs in polymer matrices is not based on exfoliation or unrolling of the nanotubes : it results in a desagglomeration process where the micrometric size agglomerates are detroyed by a slight shear force depending of the interaction between the polymer matrix and the HNT surface. This specific property can be evaluated by several tests and lead to typical classification as described in the next paragraph.

4. Fire properties/fire tests

The fire retardant properties of polymer composites are principally assessed through ignitability, flame spread, heat and smoke release [59]. These parameters are often evaluated using classically a cone calorimeter test (CCT), a UL-94 test and limiting oxygen index (LOI) test. CCT is a horizontal flame test (sample in horizontal position) while UL-94 and LOI are vertical flame tests [60]. Cone calorimetry corresponds to the oxygen consumption principle using Huggett's law, which assumes that there is a constant relationship between the quantity of oxygen consumed from the air and the amount of heat released during the sample combustion [61]. Usually specimens with dimensions of 100*100 mm^2 and a thickness of a few mm are irradiated in a horizontal position at typically 35 or 50 $kW.m^{-2}$. While plotting heat release rate (HRR) versus time , CCT gives several informations about the fire retardant properties including the time to ignition (TTI), the peak of heat release rate (PHRR), the total heat release (THR), the total smoke production (TSP) and the smoke extinction area (SEA). HRR is one of the most important parameters for characterizing the fire performance of a material as it gives informations on the fire growth and its intensity and PHRR corresponds to the maximum of the HRR curve as a function of time [62]. Moreover, the Fire Performance Index (FPI) defined as TTI/PHRR can be also of interest knowing that higher values of FPI indicate better FR performance. Another important parameter that should be calculated and interpreted regarding CCT is the global effective combustion energy (EHC = THR / ML, with ML the mass loss). Unfortunately, this EHC parameter is rarely reported in the literature.

For the LOI test, samples of 100 × 65 × 3 mm^3 are generally used when testing rigid polymers. A flame is applied to the top of the specimen until the sample is ignited. If the specimen did not ignite after 30 s, the concentration of oxygen is increased. The LOI value is the limiting concentration of oxygen at which the sample tested self-extinguishes in less than 3 min with less than 5 cm of the consumed sample. UL-94 is a polymer flammability standard. It determines the tendency of the composite to either extinguish or spread the flame once the specimen has been ignited. The specimen dimensions are 12.7 × 1.27 cm^2. The material is classified as V-2, V-1, or V-0 in increasing order of flammability rating by reference to the criteria given in Table 2.

To complete the description of these tests, some fire performances of different neat polymer matrices, as reference without any flame retardant, are reported in the Table 3.

Table 2
Classification for the rating in the UL-94 burning test.

	V-0	V-1	V-2
Burning time after flame application (s)	≤10	≤30	≤30
Total burning time (s) for 10 flame applications	≤50	≤250	≤250
Burning and afterglow times of specimens after second flame application (s)	≤30	≤60	≤60
Dripping of burning specimens (ignition of cotton batting)	No	No	Yes
Specimens completely burned	No	No	No

Table 3
Fire retardant properties of some polymer matrices; PHRR, TTI and THR.

	Irradiance ($kW.m^{-2}$)	PHRR ($kW.m^{-2}$)	TTI (s)	THR ($MJ.m^{-2}$)	UL-94	LOI (%)	Ref
Polyamide 6	50	1364±525	56±5	153±65	V-2	21-34	[44] [63]
Polyamide 12	50	724±29	47±4	78±4	V-2		[50]
Polypropylene	35	1847±238	42±12	105±14	NR[1]	18	[64][65]
Polylactide	35	369±119	69±14	77±39	NR	23	[64][66]
Epoxy	50	1052±456	58±34	58±26	NR	22.1	[67][68]
Ethylene-vinyl-acetate copolymer	35	1560±441	57±7	113±11	NR	19.5	[64][69]

[1] NR = no rating

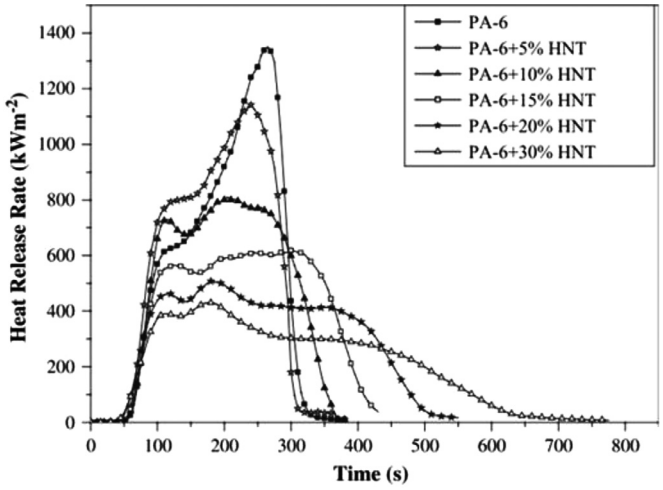

Fig. 8. Heat release rate as a function of time for PA6 and halloysite (HNTs) based composites at a heat flux of 50 kW.m^{-2} (reproduced with permission from [44] Copyright 2008, Elsevier).

5. Influence of HNT onto the fire retardancy of polymers

This chapter is dedicated to the fire properties of the HNTs based nanocomposites and the discussion will be illustrated according to the nature of the polymer from thermoplastics to thermosets.

5.1. Ignition of thermoplastics in presence of HNT

In this part, we will point out the influence of the nature of the thermoplastics on the corresponding HNT based nanocomposites fire properties. In particular, the impact of the matrix polarity on flame retardancy will be examined.

5.1.1. HNTs/PA-based composites

Polyamides are used for a wide range of applications such as electronic, electric industries, automobile or construction [70,71]. However, polyamides are relatively inflammable materials. for example, polyamides display LOI values in the range of 20-30 % [72]. Hence polyamides require being flame retarded. That is why nitrogen- and phosphorus-based additives (e.g. melamine, red phosphorus and ammonium polyphosphate APP) are widely used as FRs for polyamides [73]. These FRs have high efficiency and low toxicity. However, the use of these FRs provokes a loss of physical properties such as impact strength or thermal stability. For example, Li et al. [74] introduced 24 wt% of aluminum hypophosphite in PA6 to achieve a V-0 rating for the UL-94 test. However the tensile strength was decreased from 70MPa for the neat PA6 to 63MPa for the composite because of its high FRs amount (> 20 wt%). Therefore, nanoparticles which are known to reinforce mechanical properties of polymers were also used as flame retardants for PA. In particular, Marney et al. [44] prepared PA6 filled with 5-30 wt% of HNTs by using a twin-screw extruder at a processing temperature of 230°C. Concentrations above 15 wt% of HNT were required to improve the fire retardant property of PA6. Actually, incorporation of 15 wt% HNTs in PA6 lead to a significant change in the peak of heat release rate (PHRR, measured at irradiation of 50 kW.m^{-2}) which decreased from 1362 kW.m^{-2} (value of neat PA6) to 641 kW.m^{-2} while the LOI was slightly improved only at higher HNTs content (Fig. 8).

Indeed, they obtained a LOI of 23 % and 30 % for PA6/15 wt% HNT and PA6/30 wt% HNT, respectively, compared to 22 % for neat PA6. Halloysite nanotubes enable a thermal insulation barrier to be developed at the surface of the corresponding polymer-based composite during the burning. However, in comparison to montmorillonite-based nanocomposites, a higher amount of halloysite nanotubes was required to achieve a similar fire retardancy performance (e.g. 2-5 wt% and 15 wt%, respectively). This behavior is due to the layered silicate nature of montmorillonite which increases the formation of carboneous char and reinforced its structure thanks to the strong interaction between the decomposing polymer and the clay that exhibits larger specific surface area. Moreover the water-assisted extrusion was used to obtain a better dispersion of the HNTs as well as a better flame retardancy. Besides, Lecouvet et al. [43] showed that water injection enabled to achieve a further slight decrease in the PHRR (from 384 to 348 kW.m^{-2} for PA12 with 16 wt% HNT, measured at irradiation of 50 kW.m^{-2}). In addition, as expected, the PHRR continuously decreased with increasing the HNTs content (568 kW.m^{-2} for PA12/4 wt% HNT-W and 348 kW.m^{-2} for PA12/16 wt% HNT-W). The yield strength also increased with the HNT content and this enhancement was more pronounced for nanocomposites prepared using water injection (48MPa for neat PA12, 54MPa for PA12/16wt%HNT and 58MPa for PA12/16wt%HNT-W).

Futhermore, the incorporation of some flame-retardants into PA/HNT nanocomposites was studied in order to further improve the flame retardancy properties and to decrease the amount of HNTs. In particular, Boonkongkaew et al. [75] have described the effect of liquid bisphenol-A bis(diphenyl phosphate) (BDP, Fig. 2) onto the fire retardant properties of PA6/HNT composites. The composites were prepared using a co-rotating twin-screw extruder with a screw speed of 100 rpm and a temperature profile of 200–230°C. The content of HNTs was varied from 5 to 10 wt% and the content of BDP was varied from 2 to 4 wt%. The BDP was either loaded with the bulk polymer or partially encapsulated inside the HNTs lumen by applying vacuum prior compounding with the PA6 matrix. Indeed, the boiling point of BDP is high enough (650°C) to prevent its evaporation. The BDP encapsulation into the HNT lumen was characterized by TEM coupled with EDX analysis, TGA and FTIR. Indeed, the transparent central channel of the nanotube characterized by TEM often becomes opaque with the presence of organic molecules (e.g. BDP) into the HNT lumen. The BDP loading efficiency was evaluated by TGA using the following equation :

$$\text{Loading efficiency} = \frac{W_H - W_{H-B}}{W_H} \times 100,$$

where W_H represents the weight of the HNTs at 600°C and $W_{H\text{-}B}$ is the weight of HNT-BDP at 600°C

Considering the UL-94 vertical burning test, the incorporation of 10 wt% of HNT led to a change from V-2 for the neat polymer to V-1 for the composite. The incorporation of 4 wt% BDP in PA6 did not change the rating of UL-94. The V-0 rating was achieved by adding 10 wt% of HNT and 2 wt% of BDP directly in PA6. Moreover, it was shown that a significant decrease of PHRR (measured at irradiation of 50 kW.m^{-2}) was observed with the incorporation of HNT and BDP into PA6. The lowest PHRR value (470 kW.m^{-2}) was obtained for the nanocomposite containing 10 wt% HNT and 4 wt% BDP in which 2 wt% of BDP (quantified by TGA) was loaded into the lumen of HNTs while the PHRR of neat PA6 was 840 kW.m^{-2}. Almost the same PHRR (435 kW.m^{-2}) was obtained with 30 wt% of pristine HNTs [44]. It was suggested that BDP located in the bulk polymer operated at the beginning of the burning process while the encapsulated BDP was released over time and operated later in the combustion. Thus, there was a combined effect of HNT and BDP on the flame retardancy and the use of BDP allowed decreasing the total amount of fillers. However, thermal stability and mechanical properties are usually affected by the incorporation of both HNT and BDP. Actually, the addition of BDP in PA/HNT composite acted as a plasticizer so both the Young's modulus and the tensile strength de-

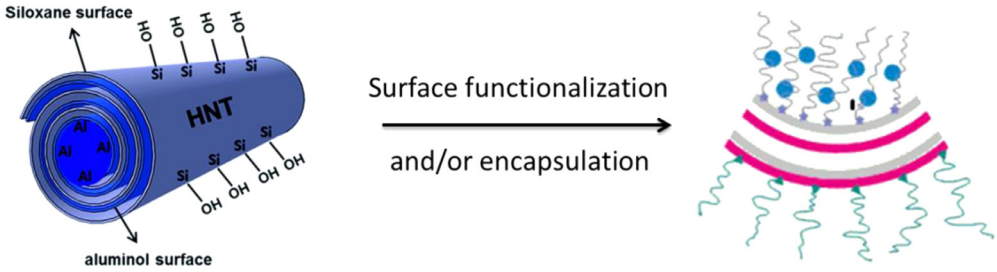

Scheme 2. Chemical compositions and functionalization of inner and outer surfaces of HNT (inspired from [78]).

Table 4
LOI values of PA6, PA6/HNT, PA6/MC and PA6/ MC/HNT nanocomposites (expressed in wt%).

Samples	LOI (%)
PA6	24.2
PA6/2HNTs	24.9
PA6/7MC	30.9
PA6/5MC/2HNTs	31.1
PA6/12MC	31.5
PA6/10MC/2HNT	31.7

creased from 2336 MPa to 2115 MPa and from 66 MPa to 55 MPa, for neat PA6 and PA6/10wt%HNT/2wt%loadedBDP/2wt%BDP, respectively. Moreover the temperature at maximum weight loss rate T_d was slightly decreased from 464°C (neat PA6) to 459°C (PA6/10wt%HNT/2wt%loadedBDP/2wt%BDP). Besides, a combinaison effect between melamine cyanurate (MC) and HNT was checked by incorporating MC in PA6/HNT nanocomposites [76,77]. HNT and MC were melt-blended with PA6 in a twin-screw extruder with a temperature profile of 200–275°C and a screw speed of 100 rpm. The amount of incorporated HNT was 2 wt% and the amount of MC was varying from 5 to 12 wt%. The LOI values of the corresponding PA6 composites increased from 24.2% (neat PA6) to 31.5% (PA6/12 wt% MC) (Table 4). Furthermore, the LOI values of PA6/HNT/MC composites, at constant weight filler contents, were almost the same (31.7 % for 12 wt% filler content (10wt%MC/2wt%HNT)).

All the nanocomposites reached the V-0 rating contrary to neat PA6 which reached the V-2 according to the UL-94 test. Unlike PA6/HNT/BDP, the mechanical properties of the PA6/HNT/MC composites were not negatively affected with a tensile strength of 59.7 MPa for PA6/2wt%HNT/10wt%MC compared to 47.8 MPa for neat PA6.

Nevertheless, to further ensure a better dispersion of HNTs in polymer matrices and/or to improve fire retardant properties of HNT-based composites, HNTs are usually chemically modified. Indeed, the presence of silanol and aluminol groups onto the outer and the inner surfaces of HNT, respectively, allows covalent grafting (scheme 2).

As a result, the outer silanol-based surface can be functionalized with alkoxy- or chloro- silanes while the inner aluminol-based surface is often modified with phosphonic acids. In particular, the surface of HNTs was chemically modified by fire retardants such as phosphorus-based compounds in order to achieve both a better dispersion in polymer matrices and an improvement of the fire-proofing. The functionalization of HNT often permits a decrease of the amount of HNTs required for enhancing flame retardancy of PA. For example, Marney et al. [61] functionalized HNTs with phenyl phosphonic acid (PPA, Fig. 2) with the help of the inner HNT aluminol groups. Nevertheless, most of the literature is based on the use of fire retardants that are inserted/encapsulated in the lumen of HNTs. In this article of Marney et al. [61], PA6/PPA-HNT nanocomposites were compounded using a twin screw extruder at a processing temperature of 220°C and a screw speed varying from 200 to 250 rpm. The dispersion of HNTs and modified HNTs (PPA-HNTs) was analyzed through X-ray mapping of elemental silicon (Fig. 9).

The HNT surface modification with PPA improved the dispersion state of HNT in PA6. Moreover, the PHRR of PA6/10wt% PPA-HNT was found to be much lower (844 $kW.m^{-2}$, measured at irradiation of 50 $kW.m^{-2}$) than the others (1890 $kW.m^{-2}$ for neat PA6 and 1296 $kW.m^{-2}$ for PA6/10wt% HNT). Nevertheless, the LOI value of PA6 (23 %) did not increase with 5 wt% PPA-HNT and it was even decreased to 21 % with 10 wt% PPA-HNT. In addition, the smoke produced by the composites containing unmodified HNTs was decreased (around 100 m^2/kg for PA6/5wt% HNT) when compared to the neat polymer (around 500 m^2/kg) while the amount of smoke produced by the composite PA6/10wt% HNT-PPA was almost doubled (around 970 m^2/kg) (Fig. 10).

It was concluded that the PPA-HNT enhanced the char formation providing a lower PHRR while PPA catalyzed the degradation of PA and consequently increased the smoke production. Another phosphorus-based compound (methyl phosphonic acid, MPA, Fig. 2), was used to functionalize the inner HNTs surface [79]. The grafting of MPA was evidenced by FTIR and by pyrolysis-gas chromatography-mass spectrometry but the amount of phosphorus grafted onto HNT was quantified by ICP. 2 wt% of P were found on Hal-P (HNT modified with MPA). 20wt% of the modified HNT (Hal-P) was incorporated into polyamide 11 (PA11) by using a twin screw extruder at a screw speed of 250 rpm with processing temperatures between 140°C and 250°C. A flat HRR (measured at irradiation of 50 $kW.m^{-2}$) curve with a PHRR of 416 $kW.m^{-2}$ was obtained for the composite whereas the HRR curve of neat PA11 was sharp with a PHRR of 977 $kW.m^{-2}$ (-57 % of PHRR for PA11/20wt% modified HNT). In the presence of the modified HNTs, a protective char layer was formed during the combustion between the polymer and the flame zone.

In addition, graphene oxide functionalized with HNTs was also used to enhance the fire-retardant properties of PA6 [80]. Graphene was used as flame retardant because of its stable structure and its capacity to form a compact dense and uniform char [81]. So, reduced graphene oxide (rGO) was decorated with halloysite nanotubes (HNTs-d-rGO, HNT/rGO 10:1 w/w) in order to minimized the needed amount of rGO, as FR in PA6. First, aminopropyltriethoxysilane (APTES, Fig. 4) was grafted to the HNTs outer surface and then it was reacted with rGO to form HNTs-d-rGO (Scheme 3).

The grafting of APTES and the decoration of rGO with HNT were evidenced by FTIR and XPS analyses but the grafted amount was not evaluated. Finally, HNTs-d-rGO (1 wt%) was mixed and melt blended with PA6 in an internal mixer at a temperature between 225 and 250°C with a screw speed of 80 rpm. The sample bearing HNTs grafted on rGO (HNTs-d-rGO) had a better dispersion in the

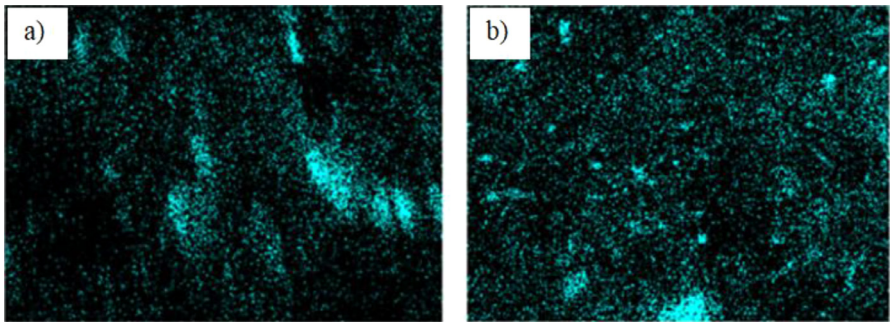

Fig. 9. X-ray mapping of PA6/HNT based composites: a) elemental silicon localization in the 10wt% HNTs composite; and b) elemental silicon localization in the 10 wt% PPA-HNTs composite (reproduced with permission from [61] Copyright 2008, Wiley).

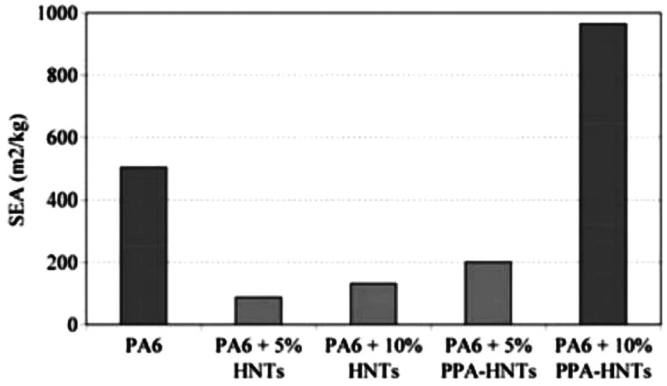

Fig. 10. Cone calorimeter (measured at irradiation of 50 kW.m^{-2}) smoke production rate in terms of smoke extinction area (SEA) for PA6, PA6/5wt%HNT, PA6/10wt%HNT, PA6/5wt%PPA-HNT and PA6/10wt%PPA-HNT composites (reproduced with permission from [61], Copyright 2012, Wiley).

PA6 matrix compared to the one obtained with a mixture of HNT and rGO. Few aggregates were observed in the last case (Fig. 11).

For a filler concentration of 1 wt%, the PHRR (measured at irradiation of 35 kW.m^{-2}) of PA6/HNTs-d-rGO was 588 kW.m^{-2} (reduced by 11 % compared to neat PA6) whereas a mixture of HNTs with GO lead to a PHRR value of 628 kW.m^{-2} (reduced by 5 %) which was attributed to the formation of a stable silicoaluminate layer on the char surface of PA6 reinforcing the barrier effect of graphene. However, it was observed that the presence of HNTs-d-rGO slightly increased the total smoke production of PA6 from 4.26 m^2/m^2 to 4.72 m^2/m^2.

The fire retardancy of polymers can also be improved by adding a protective coating layer to the polymer instead of directly incorporating the flame retardant into the polymer. Lecouvet et al. [56] prepared PA12/HNT nanocomposites as fire protective coating. These nanocomposite films were obtained by extrusion using a cast film line with temperature profile of 235–245°C. Then, the films were placed in contact with the substrate thanks to a hydraulic press at 180°C without applying additional pressure. The use of a 200 µm thickness coating of PA12/16wt%HNT onto PA12 decreased the PHRR (measured at irradiation of 50 kW.m^{-2}) value of the polymer matrix from 724 kW/m² to 529 kW/m². The PHRR value of the surface coated-samples (200 µm) with PA12/(PA12/16wt%HNT) was slightly lower than that of the nanocomposite PA12/4wt%HNT-W with HNTs directly incorporated in the polymer through water-assisted extrusion process and the char layer formed by the combustion of the composite was more continuous for the surface-coated samples (Fig. 12).

Moreover, the time to ignition was slightly increased for the coated PA12/(PA12/30wt%HNT) composite (58 s while it was 47 s for neat PA12). However, TTIwas decreased for lower HNTs content: 42s for PA12/(PA12/16wt%HNT). The authors also investigated the influence of the film thickness on the flame retardancy of the PA12/(PA12/30wt%HNT) composite. Increasing the film thickness did not lead to a change of the TTI while a decrease of the PHRR was observed. For example, the PHRR of PA12/(PA12/30wt%HNT) with a film thickness of 200 µm was 520 kW/m² while it was decreased to 362 kW/m² for a thickness of 500 µm. Nevertheless, considering the HRR curves, a critical thickness of 350 µm was observed above which there was no additional enhancement in the fire reaction (Fig. 13).

Nevertheless, it should be mentioned that when analysing the fire retardant properties of HNT-based polymer composites, the flammable polymer content is not usually considered in the literature which may moderate the HNT effect. To conclude, the fire retardant properties of polyamides can be significantly improved by incorporating HNTs into the polymer matrix (reduction of PHRR by 53 % with the addition of 15 wt% of HNT in PA6) or by elaborating a coating containing HNTs. Thanks to the good dispersion of pristine HNTs into PA, good fire retardant performances were achieved without any HNTs modification or without the use of other additives. Nevertheless, the surface modification of HNT (with methyl phosphonic acid, MPA or phenyl phosphonic acid, PPA) allows improving the fire retardancy by adding a smaller amount of fillers (reduction of the PHRR by 55 % with the addition of 10 wt% of PPA-HNT, Table 5).

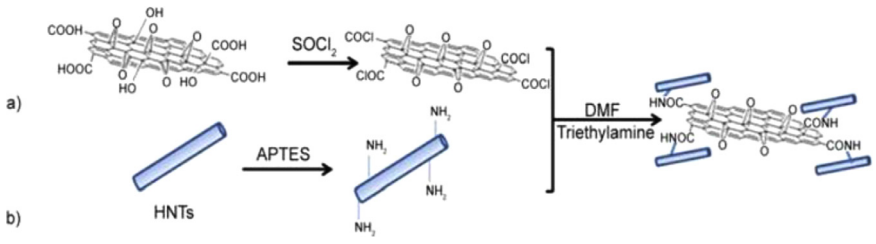

Scheme 3. Illustration of the synthetic route of HNTs-d-rGO (reproduced with permission from [80], Copyright 2014,).

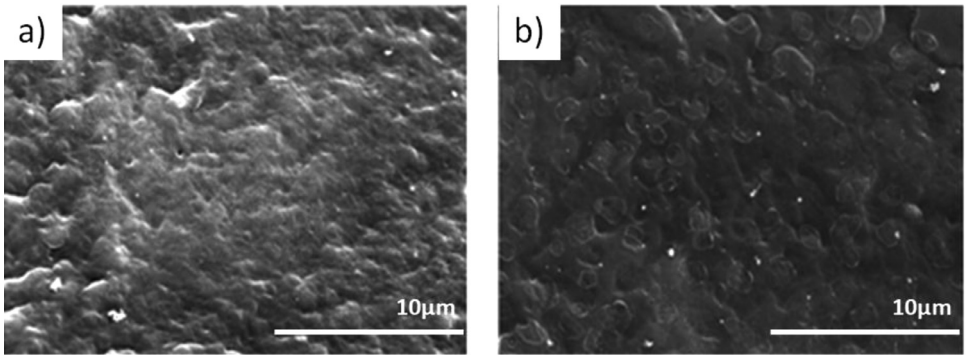

Fig. 11. SEM images obtained from fracture surface of PA6 containing 1.0 wt% of (a) HNTs-d-rGO, (b) mixture of HNTs and GO (adapted from [80]).

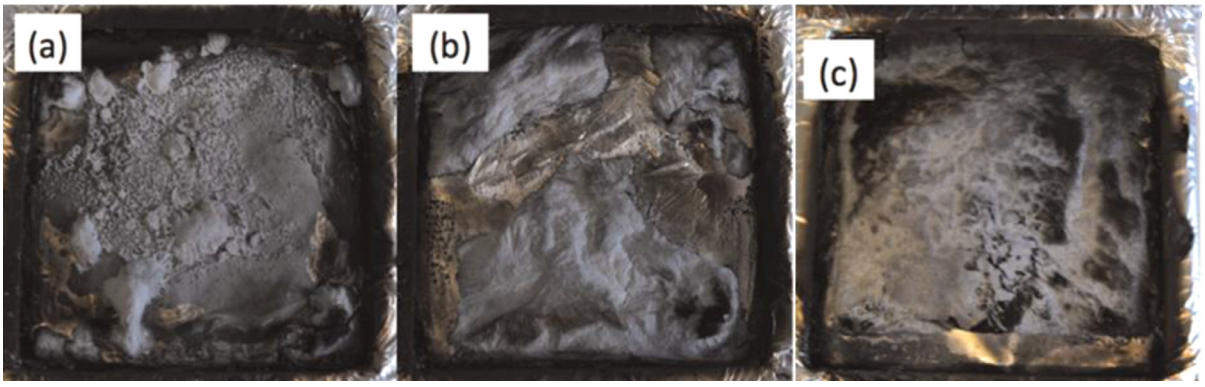

Fig. 12. Cone calorimeter residues of: (a) PA12/4wt%HNT-W, (b) PA12/(PA12/16wt%HNT 200 µm), (c) PA12/(PA12/30wt%HNT 200 µm) (reproduced with permission from [56]), Copyright, 2014) .

Table 5
Overview of the HNT/PA nanocomposites fire retardant properties (unk=unknown, not given)

Polyamide	Raw HNT (amount, wt%)	Functionalized HNT (amount, wt%)	Additives (amount, wt%)	Reduction of PHRR compared to neat polyamide (%)	Ref
PA6	15	-	0	53	[44]
PA6	10	-	BDP, 4	44	[75]
PA6		HNT-PPA, 10	0	55	[61]
PA6		HNT-d- rGO, 1	0	11	[80]
PA11		HNT-MPA[1], 20	0	57	[79]

[1] the amount of P in the MPA functionalized HNT was 2.06 wt% (measured by ICP)

5.1.2. HNTs/PLA-based composites

In the few last decades, polylactic acid/polylactide (PLA) has attracted much attention because it is bio-sourced, biodegradable and it displays a high mechanical strength. However, PLA is highly inflammable [82]. The most efficient flame retardants for PLA are halogenated compounds but these FRs are mostly classified as toxic. Nanoclays are one of the FR alternatives for PLA because they may also lead to an increase of the mechanical strength, a decrease of gas permeability and superior flame-resistance. In particular, it was demonstrated that the PHRR (measured at an irradiation of 50 $kW.m^{-2}$) of PLA nanocomposites continuously decreased with increasing HNT content (e.g. 414 $kW.m^{-2}$ for a HNT content of 8 wt% and 298 $kW.m^{-2}$ for a HNT content of 17 wt%) [53]. A further reduction in PHRR was also observed using the water-assisted extrusion process with a decrease from 298 $kW.m^{-2}$ (normal extrusion) down to 242 $kW.m^{-2}$ for the PLA/17 wt% HNTs sample obtained with water-assisted process. Moreover, Isitman et al. [83] studied the flame retardancy of polylactide nanocomposites containing aluminum phosphinate (AlPi) in presence of HNTs. The incorporation of 17 wt% of AlPi and 3 wt% of HNTs into PLA matrix using a co-rotating twin-screw extruder (temperature profile of 190–205°C with a screw speed of 85 rpm) lead to a PHRR (measured at irradiation of 35 $kW.m^{-2}$) of 511 $kW.m^{-2}$ for the PLA/17wt%AlPi/3wt%HNT composite and a PHRR of 443 $kW.m^{-2}$ for the PLA/17wt%AlPi sample. Kaya et al. [84] also obtained an increase of PHRR by incorporating 3 wt% HNTs into PLA/17 wt% AlPi matrix. In addition, HNT did not significantly affect the intumescence phenomena neither the char thickness (8.9 wt% of char residue). This behaviour was explained by both the poor dispersion of HNTs (submicrometer-sized aggregation) and their too low content (Fig. 14).

In order to improve both the dispersion of HNTs in PLA and the fire properties of the corresponding composites, Li et al. [85] prepared nanohybrids through the grafting of maleic anhydride (MAH) and 9,10-dihydro-9-oxa-10-phosphaphenanthrene-10-oxide (DOPO) onto HNT (Scheme 4).

The MAH grafting took place on both inner and outer surfaces of HNT. The grafting was evidenced by FTIR analyses and a DOPO content of 16 wt% was calculated from the thermogravimetric analysis. Then, PLA-based composites were prepared in a micro-compounder at a temperature of 165°C with a screw speed of 100 rpm for 2 min. The PLA composite with 5 wt% of HNT-MAH-DOPO showed a lower flammability than the neat PLA with a decrease of the PHRR (measured at irradiation of 35 $kW.m^{-2}$) from 397 $kW.m^{-2}$ (neat PLA) down to 317 $kW.m^{-2}$ and the time to ignition was delayed by 10 s (70 s for 5 wt% of HNT-MAH-DOPO). In

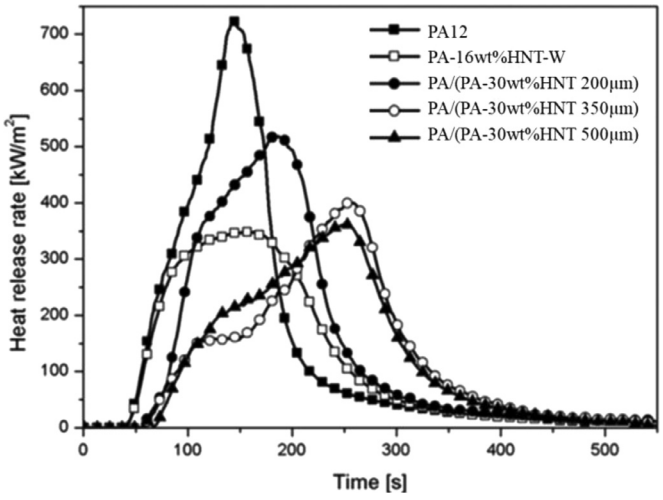

Fig. 13. Heat release rate of PA12 based-composite with various film thicknesses (adapted from [56]), measured at an irradiation of 50 kW.m^{-2}.

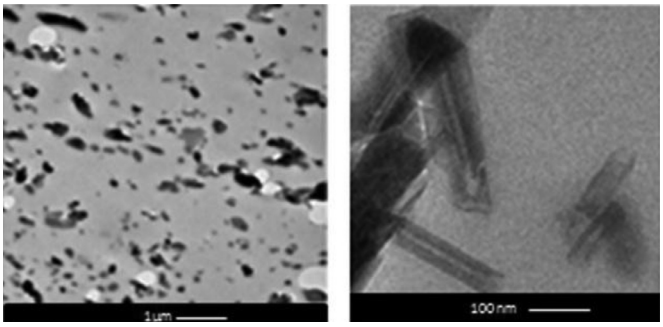

Fig. 14. TEM images of PLA/17wt%AlPi/3wt%HNT (reproduced with permission from [84], Copyright 2016).

addition, the limiting oxygen index (LOI) increased from 25 % (neat PLA) to 38 % with the addition of 5 wt% HNT-MAH-DOPO in PLA and the composite passed UL-94 vertical burning rating V-0.

In conclusion, the fire retardant properties of PLA was improved with the incorporation of HNT (reduction of 29 % in PHRR for PLA/17 wt% HNT) and further improved by a using water-assisted extrusion as process (reduction of 42% for PLA/17 wt% HNT-W). These results suggest that the improvement in dispersion results in better flame retardancy properties. Moreover, the surface modification of HNTs with MAH-DOPO allows the use of a lower HNT content and the corresponding nanocomposite still has an enhanced fire retardancy (reduction of PHRR by 20 % with 4.2 wt% HNT and 0.8 wt% MAH-DOPO).

5.1.3. HNTs/polyolefin-based composites

Polyolefins are easily inflammable because of their chemical nature so their flame retardancy is of huge importance [86]. Halloysite nanotubes are not easily dispersable in polyolefin because polyolefins are apolar polymers. Nevertheless, a significant decrease of PHRR was obtained in polypropylene/HNT composites as well as a slight improvement of LOI despite low amounts of HNT (Table 6).

Pristine HNTs were also used in combinaison with other FRs in order to improve the flame retardancy of polyolefins. For example, Sun et al. [65] introduced HNTs and kaolinite nanoplates into polypropylene containing intumescent flame retardant (IFR) composed of melamine ammonium polyphosphate (APP) and pentaerythritol phosphate with a weight ratio of 2:1. These nanocomposites were prepared by using a twin-screw extruder with a temperature profile of 170–190°C and a screw speed of 40 rpm. The addition of 25 wt% IFR into PP decreased the PHRR (measured at irradiation of 50 kW.m^{-2}) to 438 kW/m^2 which was further decreased with the addition of HNT and kaolinite (Table 7). In addition, the highest LOI value (36.9%) was measured for the PP/23.5IFR/1.5(9Kaol:1HNT) composite.

The latter composite also exhibited the best char layer quality with almost no voids (checked by TEM, Fig. 15) which was explained by a combined effect between HNT and kaolinite. Indeed, the sheets of kaolinite prevented the release of flammable gas and isolated the transfer of oxygen and external heat, while HNTs enhanced the quality of the char residue by densifying the char and making it more compact (Fig. 15c).

The surface modification of HNTs is usually done to ensure a better dispersion in polyolefins. For example, Du et al. [33] modified the HNT surface with an organosilane (γ-methacryloxy propyltrimethoxysilane, Fig. 4) before its incorporation in a PP matrix by using a twin-screw extruder, with a temperature profile of 180–200°C, and a screw speed of 100 rpm. It was observed a decrease of the number of cavities in the PP matrix and the improvement of the interface which became much blurrier (Fig. 16b). However, the fire retardant property of the nanocomposite was only slightly improved with modified HNTs. Indeed, the PHRR (measured at irradiation of 50 kW.m^{-2}) of the composites with 30 phr of modified HNTs decreased to 519 kW.m^{-2} while it was 567 kW.m^{-2} for 30 phr pristine HNTs.

Another way to improve the dispersion of HNTs in polymer matrix is to use a compatibilizer. In this way, Subasinghe et al.

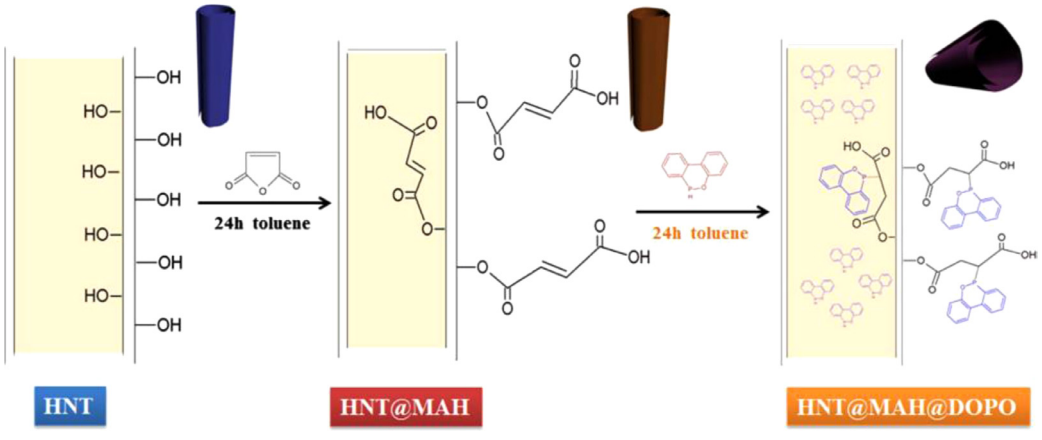

Scheme 4. Preparation route of modified HNTs with maleic anhydride and DOPO (reproduced with permission from [85], Copyright 2017, Elsevier).

Table 6
PHRR (measured at irradiation of 50 $kW.m^{-2}$) and LOI values of neat PP and PP/HNT composites.

HNT (wt%)	PHRR of the composite (PHRR of neat PP) ($kW.m^{-2}$)	LOI of the composite (LOI of neat PP) (%)	Ref
15	558 (749)		[87]
30	567 (1083)		[33]
2.5		21.3 (18.2)	[88]

Table 7
PHRR (measured at irradiation of 50 $kW.m^{-2}$) and LOI of PP and PP-based composites with HNT and kaolinite [65].

PP or PP-based composite	HNT (wt%)	Kaol (wt%)	IFR (wt%)	PHRR of the composite ($kW.m^{-2}$)	LOI of the composite (%)
PP	0	0	0	1474	18.0
PP/25IFR	0	0	25	438	31.0
PP/23.5IFR/1.5HNT	1.5	0	23.5	341	35.2
PP/23.5IFR/1.5Kaol	0	1.5	23.5	373	32.5
PP/23.5IFR/1.5(9Kaol:1HNT)	0.15	1.35	23.5	263	36.9

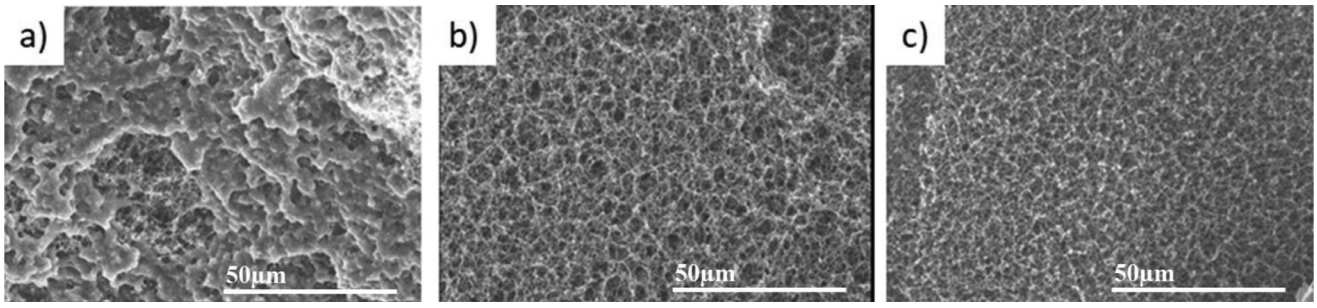

Fig. 15. SEM micrographs of the char formed after CCT: (a) 75PP/23.5IFR/1.5Kaol, (b) 75PP/23.5IFR/1.5HNT, (c) 75PP/23.5IFR/1.5(9Kaol:1HNT) (adapted from [65]).

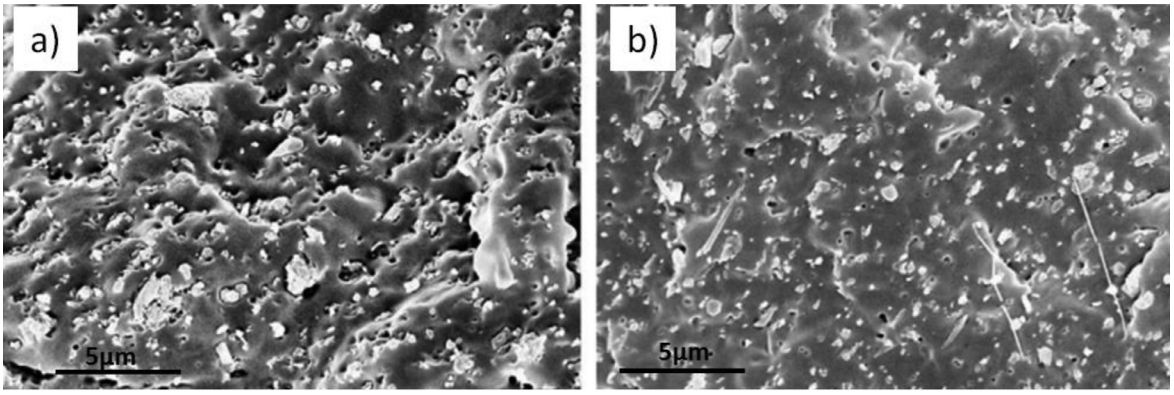

Fig. 16. SEM images of impact fractured surface of PP/HNTs composites: (a) with 30 phr of HNTs and (b) with 30 phr of γ-methacryloxy propyltrimethoxysilane modified HNTs (adapted from [33]).

[89] used PP-g-MA (3 wt%) with HNTs and ammonium polyphosphate (APP, 20 wt%) in polypropylene/kenaf fibers (Ke, 30 wt%) composite. Nanocomposites were prepared by using a twin-screw extruder with a temperature profile of 165–185°C and a screw speed of 150 rpm. The presence of APP (20 wt%) and kenaf fibers (30 wt%) into PP decreased the PHRR of the composite from 1145 $kW.m^{-2}$ down to 381 $kW.m^{-2}$ (external heat flux of 50 kW/m^2) and the addition of a low amount of HNTs (3 wt%) into the PP-Ke/APP composite did not change much the PHRR (371 $kW.m^{-2}$) while the density of the formed char residue was increased and the number of voids was lowered (Fig. 17).

As discussed above, the addition of the HNTs did not permit to decrease significantly the amount of smoke release with a maximum of smoke production of 0.06 $m^2.s^{-1}$ for PP-30Ke/20APP/3HNT while it was 0.12 $m^2.s^{-1}$ and 0.07 $m^2.s^{-1}$ for neat PP and PP-30Ke/20APP, respectively (Fig. 18).

Likewise, Jenifer et al. [88] added PP-g-MA (3 wt%) in a hybrid composite based on polypropylene, glass fiber (GF, 20 wt%) and HNTs (2.5 wt%). They used a co-rotating twin-screw extruder with a temperature profile of 160–210°C and a screw speed of 78 rpm. Considering the limiting oxygen index and the rate of burning (Table 8), it was concluded that the combination of HNT and GF allows for an improvement of fire retardant property.

Actually, the LOI was the highest (23.4 %) for the PP/20GF/2.5HNT/3PP-g-MA composite. Finally, the rate of burning was decreased from 32.5 $mm.min^{-1}$ to 19.9 $mm.min^{-1}$ for the neat PP and the latter composite, respectively. It was explained by the improvement of the HNT dispersion in presence of PP-g-MA. Indeed, HNTs formed some micro-sized aggregates in the absence of PP-g-MA (Fig. 19a) while HNTs were uniformly dispersed in PP with the addition of 3 wt% PP-g-MA (Fig. 19b).

In addition, several processes to improve the dispersion can be used at the same time. Lecouvet et al. [51,54] combined the use of a compatibilizer (PP-g-MA) and the water injection process. The best fire retardant properties were obtained for the composites containing PP-g-MA prepared with water injection according to the

Table 8
Rate of burning and LOI values for PP and PP composites with GF, HNT and PP-g-MA all three in wt% [88].

	PP	PP/20GF	PP/2.5HNT	PP/20GF/2.5HNT	PP/20GF/2.5HNT/3PP-g-MA
LOI (%)	18.2	19.1	21.3	22.2	23.4
Rate of burning[1] ($mm.min^{-1}$)	32.5	23.1	25.4	21.1	19.9

[1] For this test a flame was applied at one end of the specimen placed horizontally.

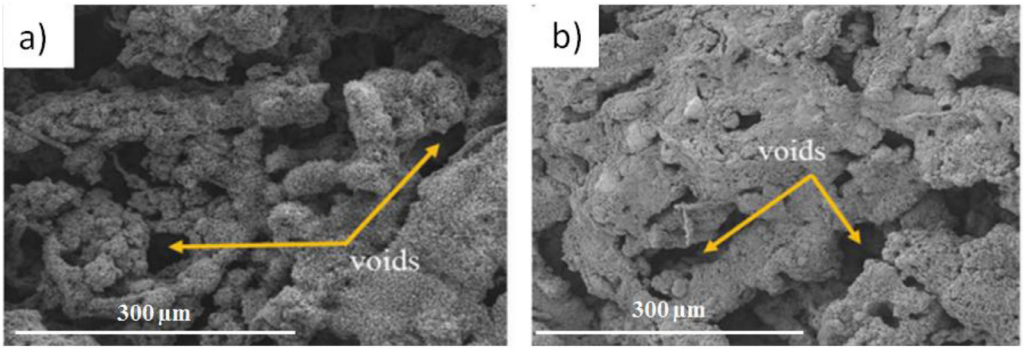

Fig. 17. SEM images of cone calorimeter char residues of PP-30Ke/20APP (a) and PP-30Ke/20APP/3HNT (b) (adapted from [89]).

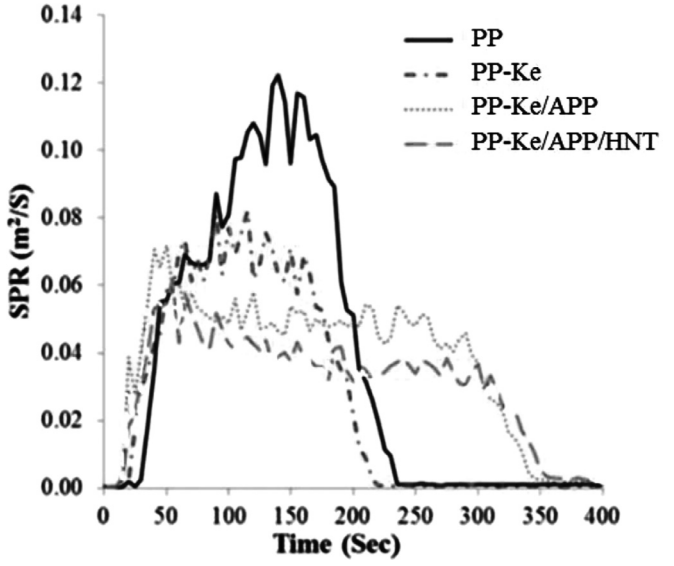

Fig. 18. Smoke release of PP and PP-based composites, PP-Ke, PP-Ke/APP and PP-Ke/APP/HNT (adapted from [89]).

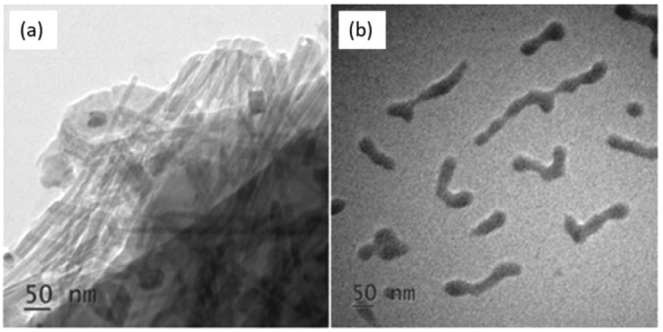

Fig. 19. TEM images of HNTs in the PP matrix (a) without PP-g-MA (PP/2.5HNT) and (b) in presence of PP-g-MA (PP/2.5HNT/3PP-g-MA) (reproduced with permission from [88], Copyright 2018, IOP Publishing Ltd).

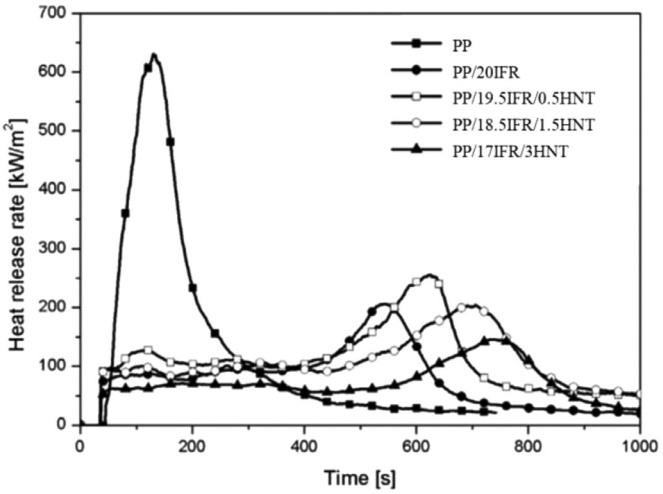

Fig. 20. Heat release rate (measured at irradiation of 50 $kW.m^{-2}$) as a function of time for neat PP and its intumescent flame retardant composites loaded at 20 wt% with different ratios of IFR and HNT (adapted from [54]).

cone calorimeter measurements. Indeed the PHRR (measured at irradiation of 50 $kW.m^{-2}$) of PP/PP-g-MA/8 wt% HNTs through the water injection process was 367 $kW.m^{-2}$ while the PHRR value for the composite without the compatibilizer was 451 $kW.m^{-2}$. They also showed that the combination of 17 wt% IFR (APP coated with a component containing nitrogenous and carbonaceous species (22 (w/w)% P, 21 (w/w)% N, 0.1 (w/w)% water)) and 3 wt% HNTs gave an important improvement in flame retardancy; the first PHRR was reduced to 63 $kW.m^{-2}$ and the heat release rate (HHR) curve was changed with the apparition of a second PHRR (145 $kW.m^{-2}$) (Fig. 20).

The first peak corresponds to the build-up of an intumescent char structure and the second peak corresponds to the char degradation at high temperature through crack formation. Jia et al. [90] used a similar approach to disperse HNT homogeneously in a PE matrix. First, graft copolymers of PE were prepared by a solid phase grafting polymerization of PE with maleic anhydride (MA), methyl methacrylate (MMA) and butyl acrylate (BA). A total grafting percentage of 12 mol% was obtained and 5 phr of the grafted copolymer was added to HNTs (10 to 60 wt%) and incorporated into LLDPE using an extrusion process at 180-200°C. It was demonstrated that the grafted copolymer enhanced the dispersion

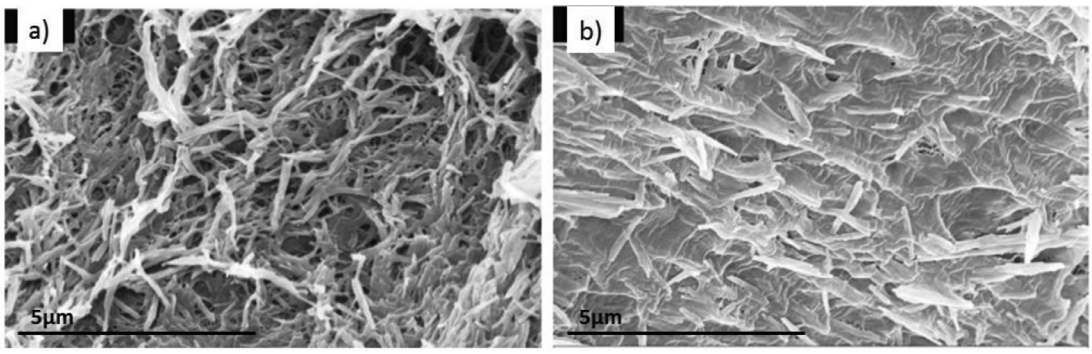

Fig. 21. SEM photographs of LLDPE/HNTs composites with and without PE-g-MA/MMA/BA. (a) LLDPE/HNTs: 100/40; (b) LLDPE/HNTs/grafted: 100/40/5 (adapted from [90]).

Table 9
Overview of the HNT/PP nanocomposites fire retardant properties.

HNT (wt%)	Additives		Total amount of fillers wt%	Reduction of PHRR compared to neat polypropylene (%)	Ref
	Nature	Amount (wt%)			
8	-	-	8	20	[51]
30	-	-	30	48	[33]
1.5	IFR (APP/PEPA)	23.5	25	77	[65]
0.15	IFR (APP/PEPA) + Kaolin	23.5 + 1.35	25	82	[65]
30	Organosilane	unk	30	52	[33]
8	PP-g-MA	10	18	20	[51]
8	PP-g-MA + water	10	18	41	[51]
3	PP-g-MA + IFR (APP)	10 + 17	30	77	[51]

of HNTs into LLDPE matrix by strengthening interfacial bonding between LLDPE and HNTs. The number of cavities and filaments on the impact fractured surface of the corresponding sample (Fig. 21b) was reduced compared to the sample without the grafted copolymer (Fig. 21a).

In addition, the PHRR of the LLDPE/40 wt%HNT/5wt% PE-g-MA/MMA/BA composite was lower (390 $kW.m^{-2}$) than LLDPE/40wt%HNT composite one (450 $kW.m^{-2}$).

In conclusion, the fire retardancy of polypropylene was significantly improved by adding a high amount of HNT (30 wt%) with a PHRR reduction of 48%. The addition of IFR (23.5 wt%) allowed a higher decrease in PHRR (-77%) with a lower amount of HNT (1.5 wt%) and a lower amount of fillers (Table 9). The use of water injection and the use of compatibilizers also allowed to improve the fire retardant properties by improving the HNTs dispersion.

5.1.4. Other thermoplastic matrices

HNTs were also used in other thermoplastic matrices such as polybutylene succinate or (acrylonitrile-butadiene-styrene) copolymer. Table 10 gives a summary of the flame retardancy properties of those polymer nanocomposites.

It can be observed that the addition of HNT into polybutylene succinate matrix decreased the PHRR of the composite while the flame retardancy was further improved by the combination of HNT with other FR (e.g. APP) with a decrease of the PHRR and a significant increase of the LOI. Likewise, the addition of HNTs (30 wt%) into ABS matrix decreased the PHRR by 38% and the combination of both HNT (10wt%) and FR (20wt%) decreased even more the PHRR by 53%.

In addition, Remanan et al. [93] studied the flammability of polymer blends of ABS and polyvinylidene fluoride (PVDF) (80/20wt%) containing 3 to 5 wt% of HNTs. ABS/PVDF/HNT composites were prepared using a micro compounder at 230°C with a screw speed of 60 rpm for 20 min. They obtained a PVDF dispersed phase into the ABS matrix with PVDF droplets of diameters ranging from 4 to 10 µm while the HNT were selectively localized in the ABS phase (Fig. 22).

Moreover, the PHRR measured by pyrolysis combustion flow calorimetry (PCFC) was considerably decreased by blending PVDF with ABS (e.g. 413.2 W/g and 547.7 W/g, respectively) while the addition of 5%wt of HNT in ABS/PVDF blend did not change significantly the PHRR. The ABS/PVDF/5wt%HNT composite exhibited the maximum char residue (11.21 %) (Fig. 23). It was concluded that this char layer acts as a thermal barrier to protect the melted polymer from the fire. The thermal behavior investigated by PCFC analysis of ABS depicted an enhancement after blending with PVDF and incorporating only 5 wt% of HNTs, which is lower than most available literature for flame retardancy (for instance 30 wt% HNT in ABS [66] and 30 wt% HNTs in PP [33] to achieve a good flame retardancy).

Saheb et al. [94] also studied some polymer blends with ABS such as PP/ABS (80/20) and they added HNT and ammonium polyphosphate/pentaerythritol (6:1 wt/wt) as IFR into PP/ABS. Moreover, PP-g-MA and styrene–ethylene, butylene–styrene triblock copolymer grafted with maleic anhydride (SEBS-g-MA) were used as compatibilizers to enhance the dispersion of the fillers. The corresponding nanocomposites were prepared by using a counter-rotating twin-screw extruder at 155–240°C with a screw speed of 10 rpm. It was observed that the number of ABS droplets increases in presence of SEBS-g-MA while their sizes decrease was attributed to a compatibilizing effect of the SEBS-g-MA (Fig. 24). Indeed, the authors stated that the formation of a SEBS-g-MA-based layer around the ABS phase prevented its coalescence.

Moreover, the addition of HNTs in PP/ABS/20IFR composite in the presence of compatibilizers increased the LOI value from 22% for the PP/ABS blend to 26.7 % for the PP/ABS/20IFR/5HNT composite. The composites with 3 wt% and 5 wt% of HNTs passed the V-2 test of UL-94 while the composite without HNTs did not. In addition, tensile and impact properties of 3wt% HNTs in 80/20 (wt/wt) PP/ABS blends in the presence of PP-MA increased slightly in comparison with the unfilled ones due to well-dispersed HNTs in the PP phase and refinement in morphology.

HNTs were also used in poly(vinyl alcohol) (PVOH) aerogel [95]. Hence, nanoscale silica, halloysite, laponite and montmorillonite were incorporated into PVOH aerogel via liquid process

Table 10
Flame retardancy of thermoplastic polymers; PHRR values are generally given at a heat flux of 50kW.m^{-2}; [a] values at 35kW.m^{-2}.

Neat polymer			FR		Processing conditions		FR properties			Ref
Matrix	LOI (%)	PHRR (kW.m^{-2})	HNT (wt%)	Added FR (wt%)	Method	Conditions	LOI (%)	PHRR (kW.m^{-2})	Residue (wt%)	
Polybutylene succinate (PBS)	-	809	10	-	Twin-screw extruder	200°C, 250 rpm	-	630	-	[91]
			5	APP (15)			-	353	-	
PBS	24.5	609	1.5	APP: melamine: pentaerythritol (4:1:1) (28.5)	Twin-screw extruder	120°C	58.2	113	32	[92]
			-	APP: melamine: pentaerythritol (4:1:1) (30)			42.1	196	13	
Acrylonitrile butadiene styrene copolymer (ABS)		1423[a]	30	-	Internal mixer	2000 rpm, 6h	-	885[a]	-	[66]
			10	APP: melamine: pentaerythritol (20)			-	673[a]	-	

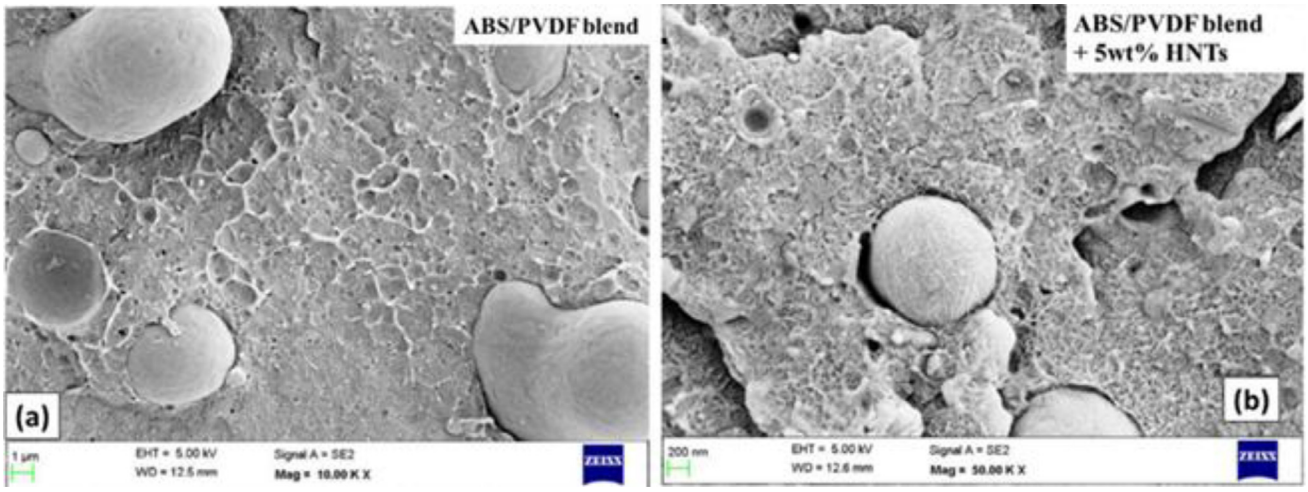

Fig. 22. SEM micrographs of different blends (a) neat ABS/PVDF (80/20) blends, (b) ABS/PVDF (80/20) blends with 5 wt% HNTs (adapted from [93]).

followed with a freeze drying method. All of the PVOH-based aerogel composites contained 5 wt% PVOH and 5 wt% inorganic nanofillers prior freezing and sublimation. The presence of inorganic nanofillers in the PVOH aerogel slightly increased the LOI of the composites (22 % for neat PVOH, 24 % for PVOH/MMT and PVOH/HNT, 25 % for PVOH/laponite and PVOH/SiO_2). The PHRR values (measured at irradiation of 50 kW.m^{-2}) of the aerogel composites with the nanofillers were considerably decreased compared with that of a neat PVOH aerogel (378 kW.m^{-2}): 121 kW.m^{-2} for PVOH/HNT and 98.6 kW.m^{-2} for PVOH/laponite, which was ascribed to the high amount of fillers (1:1 PVOH/filler). The production of CO gas was also decreased with the addition of nanofillers in PVOH aerogels (Fig. 25).

The maximum of CO production for the PVOH aerogel was 0.007 g/s while it was 0.002 g/s for the PVOH/laponite aerogels. However, at the last burning period of PVOH/HNT, a huge CO production peak occurred because of the cracking of the sample. Layered structure nanofillers had better fire retardant properties than spherical and fibrous structure nanofillers, mainly because of the enhanced barrier effects with the well organized layered structure.

HNTs were also used as FRs in ethylene-vinyl acetate copolymer (EVA). Zubkiewicz et al. [69] incorporated HNTs (2 to 8 wt%) in EVA (28wt% of VA) by a melt blending process using a counter-rotating twin-screw extruder (temperature profile of 100–145°C with a screw speed of 40 rpm). HNTs in EVA were mostly well dispersed (nanosize-scale) with the presence of some aggregates of several hundreds of nanometers. They showed that the LOI of the composites was increased with increasing concentrations of HNTs in the matrix. The LOI values were 19.5 % and 25.8 % for neat EVA and EVA/8 wt% HNTs, respectively. In addition, George et al. [96] prepared poly(ethylene-co-vinyl acetate-co-carbon monoxide) (EVACO)/HNTs (1 to 10 wt%) nanocomposite films which were solution casted in dichloromethane (DCM) as solvent. The LOI values were also improved in the presence of HNTs with LOI values of 29 % for EVACO, 31 % for EVACO/1 wt% HNT and 34 % for EVACO/10 wt%HNT.

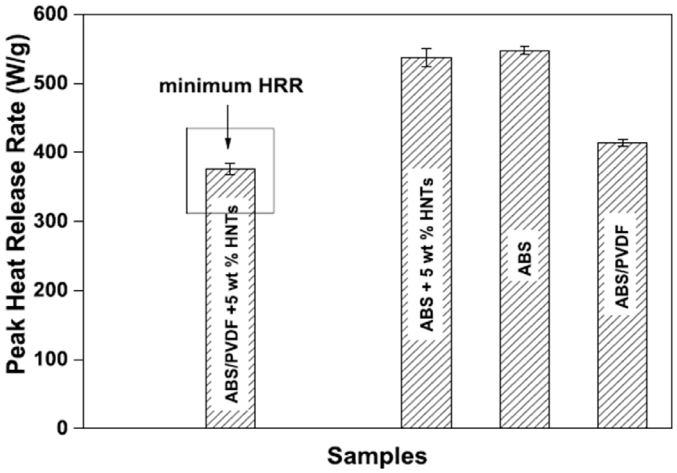

Fig. 23. Average peak heat release rate for the ABS/PVDF/HNT based composites (adapted from [93]).

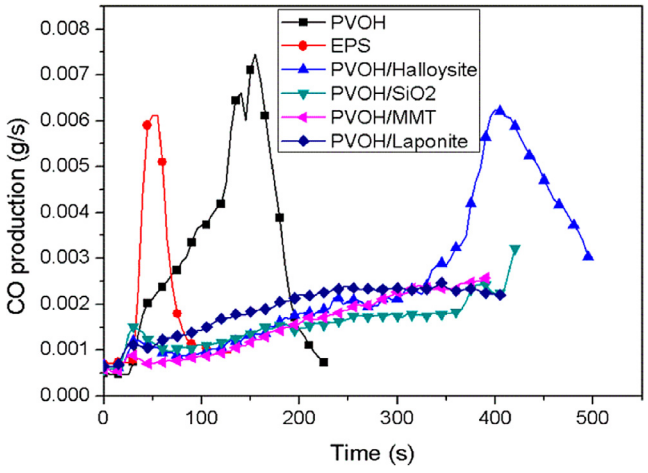

Fig. 25. CO production of aerogel PVOH, PVOH/HNT, PVOH/SiO_2, PVOH/MMT and PVOH/laponite samples as a function of the burning time (adapted from [95]).

HNTs were also used to improve the flame retardancy of polyethersulfone (PES) [97]. HNT were incorporated into PES by using water-assisted extrusion process (co-rotating twin-screw, 350°C with at a screw speed of 200 rpm and a water flow rate of 50 ml/min). The TTI was increased with the content of HNTs from 30 s (neat PES) to 65 s (PES/16wt%HNT-W). Furthermore, the PHRR value (obtained with an external heat flux of 50 kW/m^2) was significantly decreased from 130 kW.m^{-2} (neat PES) to 35 kW.m^{-2} (PES/16 wt% HNT-W) in presence of HNTs. As it can be seen from the residues obtained after mass loss calorimeter tests, the presence of the HNT lead to a more homogeneous, compact and cohesive intumescent layer (Fig. 26).

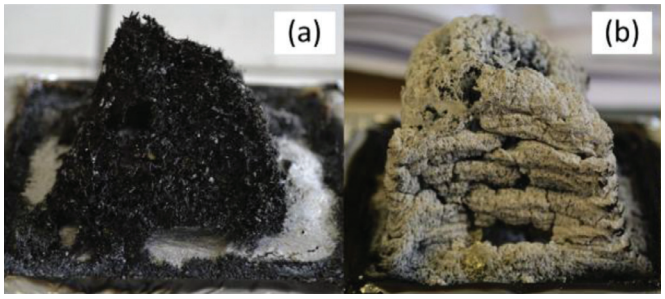

Fig. 26. Residues from cone calorimetry of: (a) neat PES and (b) PES/6wt%HNT-W nanocomposites (Reproduced with permission from [97], Copyright 2013, Elsevier).

5.2. Ignition of elastomer in presence of HNT

Elastomers and their nanocomposites have attractive properties such as physical, mechanical, thermal, and gas barrier so they are used in a wide range of applications. However, elastomers display a high flammability and therefore flame retardants are widely used in elastomers. Flame retardant elastomers include metal hydroxides, phosphorus or phosphorus/nitrogen-containing compounds. However, such FR materials require high loadings (>60 wt%) [98] so the use of nanofillers such as halloysite nanotubes in combination with other FRs were used to improve the flame retardancy while keeping low loadings and therefore good mechanical properties. Table 11 gives examples of flame retardancy properties of elastomers/HNT based nanocomposites.

Table 11 shows that elastomers containing HNTs display lower PHRR than neat elastomers and the PHRR of NBR was further lowered by combining HNT and $Mg(OH)_2$. In addition, modified HNTs with saturated aqueous iodine or bromine acid (HI, HBr) solutions and a saturated alcoholic solution of boric acid (HK) were incorporated into NBR and butadiene-styrene rubber (SBR) [101]. Iodine and bromine formed interactions with the internal hydroxyl groups of HNTs through hydrogen bonds. The modified HNTs were incor-

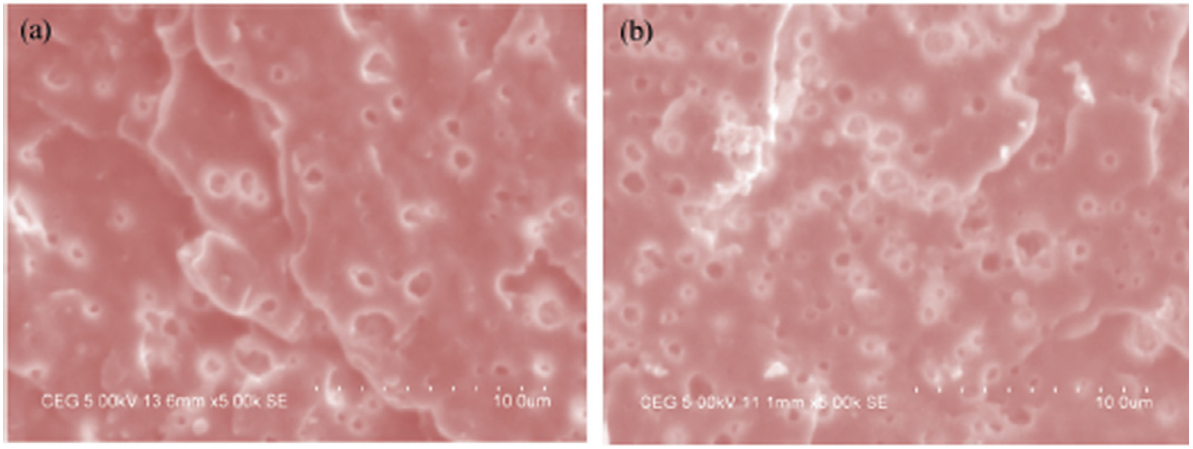

Fig. 24. SEM images of cryofractured and etched samples of (a) pure PP/ABS blend and (b) HNTs- and IFR- reinforced 80/20 (wt/wt) PP/ABS blend and their composites in the presence of PP-g-MA and SEBS-g-MA (reproduced with permission from [94], Copyright 2018).

Table 11
Flame retardancy of elastomeric polymer HNT based nanocomposites; PHRR values are given at a heat flux of 50 kW.m^{-2}.

Neat polymer Matrix	PHRR (kW.m-2)	FR HNT (wt%)	other FR (wt%)	Processing conditions Method	Conditions	FR properties LOI (%)	PHRR (kW.m-2)	Residue (wt%)	Ref
Ethylene-propylene-diene-monomer rubber copolymer (EPDM)	–	5	-	Roll mill	from 30 to 40°C	21	265.1	64	[99]
Butadiene-acrylonitrile rubber (NBR)	491.8	5	-	Roll mill	RT, 20 rpm	-	404.3	-	[100]
		5	$Mg(OH)_2$ (30)			-	81.27	-	

Table 12
Fire retardant properties of SBR composites containing 35 wt% of each filler, measured at irradiation of 35 kW.m^{-2} [103] (FPI = Fire Performance Index).

	SBR	SBR/HNT	SBR/mica	SBR/kaolin	SBR/wollastonite
PHRR (kW.m^{-1})	177	105	96	118	107
TTI (s)	34	82	61	67	51
FPI (TTI/PHRR)	0.19	0.78	0.64	0.57	0.48

porated into a rubber crosslinked in presence of dicumyl peroxide or sulfur. It was shown that the increasing content of modified HNT from 5 wt% to 15 wt% decreased the flammability of the nanocomposites, which was determined with the value of oxygen index. Considering the LOI, the best results in fire retardant properties were obtained for composites with HNTs modified with the aqueous solution of bromine (25 % for sulfur vulcanization of NBR (SNBR) with 5 wt% HNT-Br (10.21 wt% Br in HNT-Br), 23 % for SNBR with 5 wt% HNT-I and 21.5 % for SNBR with 5 wt% pristine HNT). All the composites containing modified HNTs showed a decrease in the PHRR (measured at irradiation of 35 kW.m^{-2}) compared to the neat rubber and the rubber with unmodified HNTs (e.g. 169 kW.m^{-2} and 100 kW.m^{-2} for SNBR with 5 wt% pristine HNT and SNBR with 5 wt% HNT-I, respectively). The same authors prepared hybrid fillers by the synthesis of zinc phthalocyanine (ZP) and chloroalumino phthalocyanine (CP) in presence of HNTs [102]. Phtalonitrile, zinc dust and HNT (weight ratio 8:1:4) were added together in a porcelain crucible and slowly heated up to 250°C for 60 min to obtain HNT-ZP. Phtalonitrile, anhydrous aluminum chloride and HNT (weight ratio 3:1:1.5) were heated up 300°C for 60 min to obtain HNT-CP. These fillers were incorporated (5 to 12 wt%) into NBR and SBR. Considering the LOI value, the hybrid fillers improved the fire retardant properties of the rubbers. The highest LOI values, 28.6 % and 27.8 %, were obtained for the peroxide vulcanization of NBR rubber containing 12 wt% of HNT-ZP and for the peroxide vulcanization of SBR rubber containing 12 wt% HNT-CP, respectively. In addition, lower values of PHRR (measured by PCFC) were obtained with the hybrid fillers especially in the case of NBR containing 8 wt% HNT-CP (334 W/g). Moreover, Anyszka et al. [103] investigated the fire retardant properties of SBR in the presence of 35 wt% of fillers (halloysite, calcined kaolin, mica or wollastonite). The use of 35 wt % of each filler permitted a decrease of the PHRR and an increase of the TTI (Table 12).

HNTs based composites display the highest TTI and the highest FPI in comparison with the other fillers, hence it was concluded that HNTs are the best fillers to increase the fire retardancy of SBR-based ceramizable composites increasing the FPI from 0.19 to 0.78 s.m.kW^{-1}.

5.3. Ignition of thermoset in presence of HNT

Epoxy resins (EP) are highly flammable and combustible polymers. When they are exposed to high temperatures (300-400°C), they decompose releasing smoke, heat and toxic volatiles [104]. Boron [105], phosphorus [106], and silicon [107] compounds are common flame retardant additives for EP. In addition, nano-scale additives have been used as fire retardants for EP because they can also improve their mechanical properties [108].

Flame retardant property of epoxy (diglycidyl ether of bisphenol A)/ HNT composites were studied [68, 109]. The incorporation of 3 wt% HNTs in the epoxy decreased only slightly the PHRR (reduction from 986 kW.m^{-2} down to 855 kW.m^{-2}, measured at irradiation of 50 kW.m^{-2}) but the time to ignition (TTI) was increased from 5s to 10s. Increasing the amount of HNTs to 9 wt% decreased even less the PHRR value (969 kW.m^{-2}). It was explained by the fact that the char layer formed during the combustion was not sufficiently thick and cohesive to resist against volatile degradation products; the residue was powder-like without any cohesion. The percentage of the residue after cone calorimeter was only 4.3 % for epoxy/9 wt% HNT while it was of 9.6 % for epoxy/9 wt% expandable graphite. Ammonium polyphosphate (APP) was also used as an intumescent flame retardant into the EP/modified HNT nanocomposite [68]. First, HNT were modified with an alkoxysilane (N-(2-aminoethyl)-3-aminopropyltrimethoxysilane, Fig. 4) before adding it into the polymer matrix with a three-roll mill machine in order to improve the interfacial adhesion of the HNT with the resin. The addition of 2 wt% modified HNT with 18 wt% APP (EP18A2HNT) to epoxy greatly decreased the PHRR (1910 kW.m^{-2}, 1591 kW.m^{-2}, 312.6 kW.m^{-2} and 245.5 kW.m^{-2} for neat EP, EP2HNT, EP20A and EP18A2HNT, respectively, measured at irradiation of 50 kW.m^{-2}). It exhibited a combined effect between APP and HNTs. Moreover, EP18A2HNT had a more compact char layer with smaller holes in comparison with EP20A and it achieved a V-0 rating with an improvement in the LOI (32.7 % compared to 22.1 % for neat EP) (Fig. 27).

Another FR, dimethyl methylphosphonate (DMMP), was studied in combination with HNTs into an UV-curable EP [110]. First, DMMP was incorporated into the HNT lumen under vacuum. Ac-

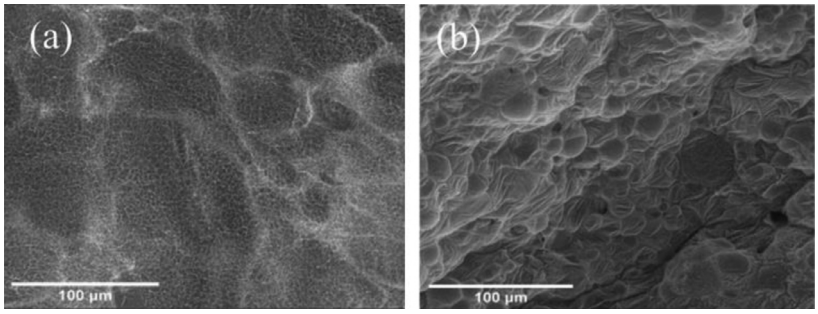

Fig. 27. SEM images of char surface for (a) EP20A and (b) EP18A2HNT after CCT test. (Reproduced with permission from [68]), Copyright 2019, Elsevier)

Table 13
Cone calorimeter data for neat EP, EP/20HNT and EP/15.2HNT-4.8DMMP, all in wt%and given for a heat flux of 50 $kW.m^{-2}$ [110].

	PHRR ($kW.m^{-2}$)	Smoke ($m^2.m^{-2}$)	Char residue (wt%)
neat EP	1002	2506	2.2
EP/20HNT	790	1777	20.9
EP/15.2HNT-4.8DMMP	578	1391	20.4

cording to TGA, the loading efficiency of DMMP, defined as the ratio between (WH-WH-D)/WH *100 where WH represents the weight of the HNTs at 800°C and WH-D is the weight of HNT-DMMP at 800°C, was 24.2 wt%. Then, 20wt%HNT-DMMP was added into EP and the blend was stirred before to be exposed to UV radiations. The PHRR value of the epoxy was decreased with the addition of pristine HNTs and it was even more decreased with the addition of HNT-DMMP (Table 13).

The total smoke release was also significantly decreased with the addition of HNT-DMMP and the char residue mass of EP/HNT-DMMP (20.4 wt%) was almost equal to that of EP/20HNT (20.9 wt%). However, the surface of this char layer was flatter and more compact than that of EP/HNT which was explained by the improvement of the stability of the combustion residues in presence of HNT-DMMP. The flame retardant mechanism of HNT-DMMP consisted of first the gasification of DMMP and then the formation of a polyphosphoric-HNT carbon layer in the condensed phase.

In addition, Ferrum ammonium phosphate ($FeNH_4PO_4$, FAP)-HNTs and an intumescent flame retardant OP ($[C_4H_{10}PO_2]_3Al$) were incorporated into an epoxy resin to prepare polymer nanocomposites [111]. The epoxy was a difunctional bisphenol A/epichlorohydrin derived liquid epoxy resin. FAP was used for its flame retardant properties and its effectiveness for wastewater treatment. FAP-HNTs (1:1 w/w) were prepared by an adsorption-precipitation method through an immersion in EP resin without stirring for 24h followed by the addition of OP. It was observed that the PHRR of neat epoxy (400 W/g), obtained by pyrolysis combustion flow calorimetry, decreased by the addition of 20 wt% of FAP (236 W/g) while no combined effect was observed by adding HNT (269 W/g and 244 W/g for 20 wt%FAP-HNT and 10wt%FAP-HNT/10OP, respectively). Nevertheless, the use of a cone calorimeter would probably highlight a HNT effect on HRR. In addition, the EP/10FAP–HNT/10OP passed the UL 94 V-0 rating. The EDS analysis of the char revealed that EP/10FAP-HNT/10OP had higher carbon content (13.1 wt%) and lower oxygen (43.4 wt%) content than EP/20FAP-HNT (11.8 wt% C and 48 wt% O) which indicated better char forming performance.

Another system of flame retardancy containing HNTs into an epoxy matrix (composed of bisphenol A and epoxy chloropropane) was studied. This system was composed of HNT as nanofiller, chitosan (CS) as char-forming agent and ferrosoferric oxide as a char catalyst (HNT-CS-Fe_3O_4) [112]. CS was absorbed outside HNTs because of the positively charged amino group of CS which could be combined with the negative charge onto the outer surface of HNTs by electrostatic interactions. The weight percentages of CS and Fe_3O_4 in HNT-CS-Fe_3O_4 were calculated from TGA analysis (8 wt% and 31 wt%, respectively) and the nanocomposites were prepared by a liquid-phase route. EP and HNT-CS-Fe_3O_4 were stirred together with a vacuum mixer at 1600 rpm for 5 min and then dried at 80°C. The LOI of neat epoxy was 21.1 % and the addition of 10 wt% HNT increased the LOI value to 23.8 % while the addition of 10 wt% modified HNT (HNT-CS-Fe_3O_4) increased more significantly the LOI value to 31.3 %. The HRR curves of neat EP and EP/10wt%HNT were sharp (intense burning), while HRR curve of EP/10wt% HNT-CS-Fe_3O_4 was flat. Moreover the PHRR value of EP (measured at irradiation of 35 $kW.m^{-2}$) decreased from 865 $kW.m^{-2}$ for pure EP to 589 $kW.m^{-2}$ for EP/10HNT-CS-Fe_3O_4. Nevertheless, the total smoke production rate was more important for EP/10HNT-CS-Fe_3O_4 (3301 $m^2.m^{-2}$) than for EP/10HNT (2869 $m^2.m^{-2}$). Unlike the other EP nanocomposites, EP/10HNT-CS-Fe_3O_4 composite produced a continuous and dense residual char layer (Fig. 28).

According to laser Raman spectroscopy, the ratio of I_D/I_G (D peak at 1352cm^{-1} and G peak at 1596 cm^{-1}) was used to describe the degree of graphitization of char residue. EP/HNT-CS-Fe_3O_4 composite had the lowest ratio of I_D/I_G (2.4 while it was 3.1 for neat EP) suggesting that this composite had a better degree of graphitization of char residue than the other studied composites.

Besides, the technique based on a HNT protective coating was used to improve the fire retardancy of polyurethane. Wu et al. [113] coated a polyurethane foam (PUF) with HNTs by using a dip coating process. First, HNTs were modified by surface grafting with triethoxysilane and then with hexadecyltrimethoxysilane (15.9 wt% grafted alkoxysiloxane) in order to obtain superhydrophobic HNTs ensuring oil absorption. The flame retardancy of the modified PUF was assessed by an open flame test. The presence of modified HNTs in PUF diminished its flammability and the nanocomposite self-extinguished at HNT contents of 8 wt%. Moreover, the presence of HNTs increased the LOI from 19 % for PUF to 23 % for PUF coated with 6 wt% of modified HNTs. In addition, Smith et al. [114] developed multilayered HNT based nanocomposite coatings. They coated PUF by 3 to 5 successive layers of branched polyethylenimine (BPEI)-HNT and poly(acrylic acid) (PAA)-HNT. HNTs (0.5 wt%) were dispersed in 0.1 wt% PAA solutions and 0.1 wt% BPEI solutions. Then the solutions were used for dip-coating. According to

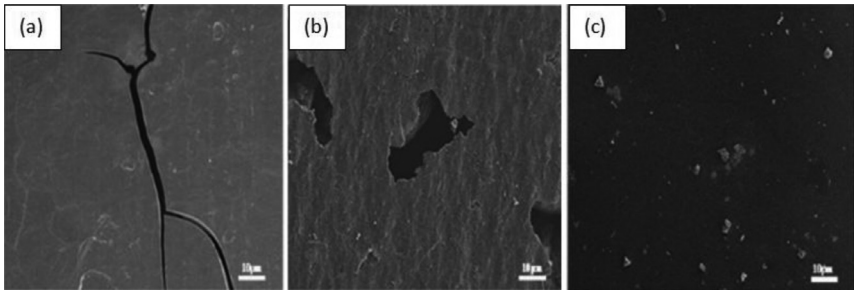

Fig. 28. SEM images of the inner surfaces of char residues of (a) EP, (b) EP/10HNT and (c) EP/10HNT-CS-Fe_3O_4 after CCT (reproduced with permission from [112], Copyright 2019).

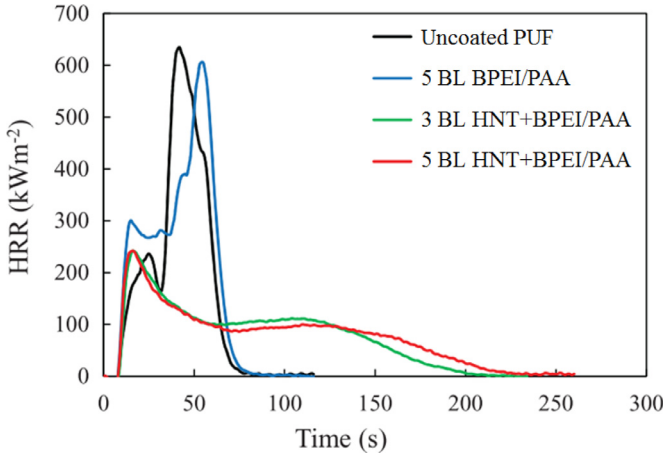

Fig. 29. Heat release rate curves for coated and uncoated polyurethane foam. BL=bilayer (reproduced with permission from [114], Copyright 2018).

TGA, HNT content in the 3 and 5 bilayers coatings was 91 and 86 wt%, respectively. Then, cone calorimeter analyses were conducted with a heat flux of 35 $kW.m^{-2}$ and the presence of 5 bilayers of BPEI/PAA onto PUF had only a very slight influence on the PHRR (621 $kW.m^{-2}$ against 634 $kW.m^{-2}$ for uncoated PUF) whereas the presence of only 3 bilayers of BPEI-HNT/PAA-HNT (total thickness of 195 nm) significantly decreased the PHRR to 244 $kW.m^{-2}$ (reduction of 61 %). Therefore, there was no significant difference in PHRR by increasing the number of bilayers containing HNTs (Fig. 29).

Nevertheless, 5 bilayers allowed increasing the reduction of the total smoke release: 60 % of reduction for 5 bilayers (71 $m^2.m^{-2}$) and 48% for 3 bilayers (93 $m^2.m^{-2}$). Moreover, according to open flame testing the foam self-extinguished before the flame spread over the entire surface with a 5 bilayers HNT.

6. Conclusions

Halloysite nanotubes are often used to improve the flame retardancy of polymer nanocomposites. HNT can act as a flame retardant agent by forming both a ceramic like structure and a barrier against heat and mass transport. However, it is only efficient if the processing parameters are optimized in order to achieve a good dispersion of HNT in the polymer system. Flame retardant (FR) molecules can be encapsulated into the lumen while its silanol-containing surface can be functionalized to ensure a better dispersion in polymer matrices. Increase in HNT concentration resulted in an improvement of the flame retardancy of the corresponding nanocomposite with polymers as well as its synergy with the use of other flame retardants. The incorporation of HNTs in polymer matrices allows for good fire retardancy properties in the content range 3wt%-20wt% depending on the polymer nature.

Declaration of Competing Interest

The authors declare that they have no known competing financial interests or personal relationships that could have appeared to influence the work reported in this paper.

Aknowledgments

The French National Agency for Research (ANR-18-CE06-0020-03) for funding and the competitiveness cluster Axelera.

This manuscript is a tribute to the 50 year anniversary of the French Polymer Group (Groupement Français des Polymères - GFP).

References

[1] C. Wilkie, A. Morgan (Eds.), Fire Retardancy of Polymeric Materials, CRC Press, 2009, doi:10.1201/9781420084009.
[2] A. Dasari, Z.Z. Yu, G.P. Cai, Y.W. Mai, Recent developments in the fire retardancy of polymeric materials, Prog. Polym. Sci. 38 (2013) 1357–1387, doi:10.1016/j.progpolymsci.2013.06.006.
[3] F. Carosio, A. Di Blasio, F. Cuttica, J. Alongi, A. Frache, G. Malucelli, Flame retardancy of polyester fabrics treated by spray-assisted layer-by-layer silica architectures, Ind. Eng. Chem. Res. 52 (2013) 9544–9550, doi:10.1021/ie4011244.
[4] N. Levinţa, Z. Vuluga, M. Teodorescu, M.C. Corobea, Halogen-free flame retardants for application in thermoplastics based on condensation polymers, SN Appl. Sci. 1 (2019), doi:10.1007/s42452-019-0431-6.
[5] L. Wan, C. Deng, Z.Y. Zhao, H. Chen, Y.Z. Wang, Flame retardation of natural rubber: Strategy and recent progress, Polymers (Basel) 12 (2020), doi:10.3390/polym12020429.
[6] M.J. Xu, Y. Ma, M.J. Hou, B. Li, Synthesis of a cross-linked triazine phosphine polymer and its effect on fire retardancy, thermal degradation and moisture resistance of epoxy resins, Polym. Degrad. Stab. 119 (2015) 14–22, doi:10.1016/j.polymdegradstab.2015.04.027.
[7] S.V. Levchik, E.D. Weil, A review of recent progress in phosphorus-based flame retardants, J. Fire Sci 24 (2006) 345–364, doi:10.1177/0734904106068426.
[8] M.M. Alam, B. Biswas, A.K. Nedeltchev, H. Han, A.D. Ranasinghe, P.K. Bhowmik, K. Goswami, Phosphine oxide containing poly(pyridinium salt)s as fire retardant materials, Polymers (Basel) 11 (2019), doi:10.3390/polym11071141.
[9] J. Green, A Review of Phosphorus- Containing Flame Retardants, J. Fire Sci 14 (1996) 353–366.
[10] G. Woodward, C. Harris, J. Manku, Design of new organophosphorus flame retardants, Phosphorus, Sulfur Silicon Relat. Elem. 144–146 (1999) 25–28, doi:10.1080/10426509908546173.
[11] E.D. Weil, S.V. Levchik, M. Ravey, W. Zhu, A survey of recent progress in phosphorus-based flame retardants and some mode of action studies, Phosphorus, Sulfur Silicon Relat. Elem. 144–146 (1999) 17–20, doi:10.1080/10426509908546171.
[12] Z. Czégény, M. Blazsó, Effect of phosphorous flame retardants on the thermal decomposition of vinyl polymers and copolymers, J. Anal. Appl. Pyrolysis. 81 (2008) 218–224, doi:10.1016/j.jaap.2007.11.005.
[13] J. Green, A Phosphorus-Bromine Flame Retardant for Engineering Thermoplastics—A Review, J. Fire Sci 12 (1994) 388–408, doi:10.1177/073490419401200404.
[14] S.-Y. Lu, I. Hamerton, Recent developments in the chemistry of halogen-free flame retardant polymers, Prog. Polym. Sci. 27 (2002) 1661–1712.

[15] H. Horacek, R. Grabner, Advantages of flame retardants based on nitrogen compounds, Polym. Degrad. Stab. 54 (1996) 205–215, doi: 10.1016/s0141-3910(96)0 0 045-6.

[16] R.N. Rothon, P.R. Hornsby, Flame retardant effects of magnesium hydroxide, Polym. Degrad. Stab. 54 (1996) 383–385, doi:10.1016/s0141-3910(96)00067-5.

[17] S. Bourbigot, M. Le Bras, F. Dabrowski, J.W. Gilman, T. Kashiwagi, PA-6 clay nanocomposite hybrid as char forming agent in intumescent formulations, Fire Mater 24 (2000) 201–208, doi:10.1002/1099-1018(200007/08)24:4⟨201::AID-FAM739⟨3.0.CO;2-D.

[18] S. Bourbigot, M. Le Bras, S. Duquesne, M. Rochery, Recent advances for intumescent polymers, Macromol. Mater. Eng. 289 (2004) 499–511, doi:10.1002/mame.200400007.

[19] A .B. Shehata, M.A. Hassan, N.A. Darwish, Kaolin modified with new resin-iron chelate as flame retardant system for polypropylene, J. Appl. Polym. Sci. 92 (2004) 3119–3125, doi: 10.1002/app.20226.

[20] N.F. Attia, N.S. Abd El-Aal, M.A. Hassan, Facile synthesis of graphene sheets decorated nanoparticles and flammability of their polymer nanocomposites, Polym. Degrad. Stab. 126 (2016) 65–74, doi: 10.1016/j.polymdegradstab.2016. 01.017.

[21] B. Dittrich, K.A. Wartig, D. Hofmann, R. Mülhaupt, B. Schartel, Carbon black, multiwall carbon nanotubes, expanded graphite and functionalized graphene flame retarded polypropylene nanocomposites, Polym. Adv. Technol. 24 (2013) 916–926, doi: 10.1002/pat.3165.

[22] T. Kashiwagi, F. Du, K.I. Winey, K.M. Groth, J.R. Shields, S.P. Bellayer, H. Kim, J.F. Douglas, Flammability properties of polymer nanocomposites with single-walled carbon nanotubes: Effects of nanotube dispersion and concentration, Polymer (Guildf) 46 (2005) 471–481, doi:10.1016/j.polymer.2004.10.087.

[23] A. Fina, G. Camino, S. Bocchini, Comprehensive Approach to Flame-Retardancy Evaluation of Layered Silicate Nanocomposites, in: Polym. Green Flame Retard., Elsevier, 2014, pp. 441–459, doi:10.1016/B978-0-444-53808-6.00014-7.

[24] G. Beyer, Nanocomposites: A new class of flame retardants for polymers, Plast. Addit. Compd. 4 (2002) 22–28, doi: 10.1016/S1464-391X(02)80151-9.

[25] P. Kiliaris, C.D. Papaspyrides, Polymer/layered silicate (clay) nanocomposites: An overview of flame retardancy, Prog. Polym. Sci. 35 (2010) 902–958, doi: 10.1016/j.progpolymsci.2010.03.001.

[26] G. Beyer, Flame retardant properties of EVA-nanocomposites and improvements by combination of nanofillers with aluminium trihydrate, Fire Mater 25 (2001) 193–197, doi: 10.1002/fam.776.

[27] M. Liu, Z. Jia, D. Jia, C. Zhou, Recent advance in research on halloysite nanotubes-polymer nanocomposite, Prog. Polym. Sci. 39 (2014) 1498–1525, doi:10.1016/j.progpolymsci.2014.04.004.

[28] P. Yuan, D. Tan, F. Annabi-Bergaya, Properties and applications of halloysite nanotubes: Recent research advances and future prospects, Appl. Clay Sci. 112–113 (2015) 75–93, doi:10.1016/j.clay.2015.05.001.

[29] G. Cavallaro, L. Chiappisi, P. Pasbakhsh, M. Gradzielski, G. Lazzara, A structural comparison of halloysite nanotubes of different origin by Small-Angle Neutron Scattering (SANS) and Electric Birefringence, Appl. Clay Sci. 160 (2018) 71–80, doi:10.1016/j.clay.2017.12.044.

[30] A. Kausar, Review on Polymer/Halloysite Nanotube Nanocomposite, Polym. - Plast. Technol. Eng. 57 (2018) 548–564, doi:10.1080/03602559.2017.1329436.

[31] P. Pasbakhsh, G.J. Churchman, J.L. Keeling, Characterisation of properties of various halloysites relevant to their use as nanotubes and microfibre fillers, Appl. Clay Sci. 74 (2013) 47–57, doi: 10.1016/j.clay.2012.06.014.

[32] M. Makaremi, P. Pasbakhsh, G. Cavallaro, G. Lazzara, Y.K. Aw, S.M. Lee, S. Milioto, Effect of Morphology and Size of Halloysite Nanotubes on Functional Pectin Bionanocomposites for Food Packaging Applications, ACS Appl. Mater. Interfaces. 9 (2017) 17476–17488, doi:10.1021/acsami.7b04297.

[33] M. Du, B. Guo, D. Jia, Thermal stability and flame retardant effects of halloysite nanotubes on poly(propylene), Eur. Polym. J. 42 (2006) 1362–1369, doi: 10.1016/j.eurpolymj.20 05.12.0 06.

[34] L. Liu, Y. Wan, Y. Xie, R. Zhai, B. Zhang, J. Liu, The removal of dye from aqueous solution using alginate-halloysite nanotube beads, Chem. Eng. J. 187 (2012) 210–216, doi:10.1016/j.cej.2012.01.136.

[35] M. Du, B. Guo, D. Jia, Newly emerging applications of halloysite nanotubes: A review, Polym. Int. 59 (2010) 574–582, doi:10.1002/pi.2754.

[36] M. Liu, Y. Zhang, C. Wu, S. Xiong, C. Zhou, Chitosan/halloysite nanotubes bionanocomposites: Structure, mechanical properties and biocompatibility, Int. J. Biol. Macromol. 51 (2012) 566–575, doi:10.1016/j.ijbiomac.2012.06.022.

[37] C.I. Idumah, A. Hassan, J. Ogbu, J.U. Ndem, I.C. Nwuzor, Recently emerging advancements in halloysite nanotubes polymer nanocomposites, Compos. Interfaces. 26 (2019) 751–824, doi:10.1080/09276440.2018.1534475.

[38] F. Najihah, N. Mohd, R. Abdul, N. Attan, Nanocellulose and nanoclay as reinforcement materials in polymer composites : A review, 16 (2020) 145–153.

[39] K. Prashantha, H. Schmitt, M.F. Lacrampe, P. Krawczak, Mechanical behaviour and essential work of fracture of halloysite nanotubes filled polyamide 6 nanocomposites, Compos. Sci. Technol. 71 (2011) 1859–1866, doi: 10.1016/j.compscitech.2011.08.019.

[40] L.N. Carli, J.S. Crespo, R.S. Mauler, PHBV nanocomposites based on organomodified montmorillonite and halloysite: The effect of clay type on the morphology and thermal and mechanical properties, Compos. Part A Appl. Sci. Manuf. 42 (2011) 1601–1608, doi: 10.1016/j.compositesa.2011.07.007.

[41] T.S. Gaaz, A.B. Sulong, A.A.H. Kadhum, A.A. Al-Amiery, M.H. Nassir, A.H. Jaaz, The impact of halloysite on the thermo-mechanical properties of polymer composites, Molecules 22 (2017) 13–15, doi:10.3390/molecules22050838.

[42] I. Kaygusuz, C. Kaynak, Influences of halloysite nanotubes on crystallisation behaviour of polylactide, Plast. Rubber Compos. 44 (2015) 41–49, doi:10.1179/1743289814Y.0000000116.

[43] M. Il Kim, S. Kim, T. Kim, D.K. Lee, B. Seo, C.S. Lim, Mechanical and thermal properties of epoxy composites containing zirconium oxide impregnated halloysite nanotubes, Coatings 7 (2017), doi:10.3390/coatings7120231.

[44] D.C.O. Marney, L.J. Russell, D.Y. Wu, T. Nguyen, D. Cramm, N. Rigopoulos, N. Wright, M. Greaves, The suitability of halloysite nanotubes as a fire retardant for nylon 6, Polym. Degrad. Stab. 93 (2008) 1971–1978, doi:10.1016/j.polymdegradstab.2008.06.018.

[45] T. Zheng, X. Ni, Loading an organophosphorous flame retardant into halloysite nanotubes for modifying UV-curable epoxy resin, RSC Adv. 6 (2016) 57122–57130, doi:10.1039/c6ra08178a.

[46] T. Kashiwagi, E. Grulke, J. Hilding, R. Harris, W. Awad, J. Douglas, Thermal degradation and flammability properties of poly(propylene)/carbon nanotube composites, Macromol. Rapid Commun. 23 (2002) 761–765, doi:10.1002/1521-3927(20020901)23:13⟨761::AID-MARC761⟨3.0.CO;2-K.

[47] J. Zhu, F.M. Uhl, A.B. Morgan, C.A. Wilkie, Studies on the mechanism by which the formation of nanocomposites enhances thermal stability, Chem. Mater. 13 (2001) 4649–4654, doi:10.1021/cm010451y.

[48] E.S. Goda, K.R. Yoon, S.H. El-sayed, S.E. Hong, Halloysite nanotubes as smart flame retardant and economic reinforcing materials: A review, Thermochim. Acta 669 (2018) 173–184, doi:10.1016/j.tca.2018.09.017.

[49] K. Szpilska, K. Czaja, S. Kudła, Thermal stability and flammability of polyolefin/halloysite nanotubes composites, Polimery/Polymers 60 (2015) 673–679, doi:10.14314/polimery.2015.673.

[50] B. Lecouvet, M. Sclavons, S. Bourbigot, C. Bailly, Towards scalable production of polyamide 12/halloysite nanocomposites via water-assisted extrusion: Mechanical modeling, thermal and fire properties, Polym. Adv. Technol. 25 (2014) 137–151, doi:10.1002/pat.3215.

[51] B. Lecouvet, M. Sclavons, S. Bourbigot, J. Devaux, C. Bailly, Water-assisted extrusion as a novel processing route to prepare polypropylene/halloysite nanotube nanocomposites: Structure and properties, Polymer (Guildf) 52 (2011) 4284–4295, doi:10.1016/j.polymer.2011.07.021.

[52] Z. Jia, Y. Luo, B. Guo, B. Yang, M. Du, D. Jia, Reinforcing and flame-retardant effects of halloysite nanotubes on LLDPE, Polym. - Plast. Technol. Eng. 48 (2009) 607–613, doi:10.1080/03602550902824440.

[53] G. Stoclet, M. Sclavons, B. Lecouvet, J. Devaux, P. Van Velthem, A. Boborodea, S. Bourbigot, N. Sallem-Idrissi, Elaboration of poly(lactic acid)/halloysite nanocomposites by means of water assisted extrusion: Structure, mechanical properties and fire performance, RSC Adv. 4 (2014) 57553–57563, doi:10.1039/c4ra06845a.

[54] B. Lecouvet, M. Sclavons, C. Bailly, S. Bourbigot, A comprehensive study of the synergistic flame retardant mechanisms of halloysite in intumescent polypropylene, Polym. Degrad. Stab. 98 (2013) 2268–2281, doi:10.1016/j.polymdegradstab.2013.08.024.

[55] W.Y. Zhou, B. Guo, M. Liu, R. Liao, A.B.M. Rabie, D. Jia, Poly(vinyl alcohol)/Halloysite nanotubes bionanocomposite films: Properties and in vitro osteoblasts and fibroblasts response, J. Biomed. Mater. Res. - Part A. 93 (2010) 1574–1587, doi:10.1002/jbm.a.32656.

[56] B. Lecouvet, M. Sclavons, S. Bourbigot, C. Bailly, Highly loaded nanocomposite films as fire protective coating for polymeric substrates, J. Fire Sci 32 (2014) 145–164, doi:10.1177/0734904113500207.

[57] W. Wei, E. Abdullayev, A. Hollister, D. Mills, Y.M. Lvov, Clay nanotube/poly(methyl methacrylate) bone cement composites with sustained antibiotic release, Macromol. Mater. Eng. 297 (2012) 645–653, doi:10.1002/mame.201100309.

[58] Y. Lvov, E. Abdullayev, Functional polymer-clay nanotube composites with sustained release of chemical agents, Prog. Polym. Sci. 38 (2013) 1690–1719, doi:10.1016/j.progpolymsci.2013.05.009.

[59] S. Levchik, Introduction To Flame Flammability, Flame Retard. Polym. Nanocomposites (2006) 1–30, doi:10.1002/0470109033.

[60] S. Bourbigot, S. Duquesne, Fire retardant polymers: Recent developments and opportunities, J. Mater. Chem. 17 (2007) 2283–2300, doi:10.1039/b702511d.

[61] D.C.O. Marney, W. Yang, L.J. Russell, S.Z. Shen, T. Nguyen, Q. Yuan, R. Varley, S. Li, Phosphorus intercalation of halloysite nanotubes for enhanced fire properties of polyamide 6, Polym. Adv. Technol. 23 (2012) 1564–1571, doi:10.1002/pat.3030.

[62] A. Tewarson, Heat release rate in fires, Fire Mater 4 (1980) 185–191, doi:10.1002/fam.810040405.

[63] M. Gilbert, Relation of Structure to Chemical Properties, Brydson's Plast. Mater. Eighth Ed. (2017) 75–102, doi:10.1016/B978-0-323-35824-8.00005-0.

[64] H. Vahabi, B.K. Kandola, M.R. Saeb, Flame Retardancy Index for thermoplastic composites, Polymers (Basel) 11 (2019) 1–10, doi:10.3390/polym11030407.

[65] W. Sun, W. Tang, X. Gu, S. Zhang, J. Sun, H. Li, X. Liu, Synergistic effect of kaolinite/halloysite on the flammability and thermostability of polypropylene, J. Appl. Polym. Sci. 135 (2018) 1–8, doi:10.1002/app.46507.

[66] N.F. Attia, M.A. Hassan, M.A. Nour, K.E. Geckeler, Flame-retardant materials: Synergistic effect of halloysite nanotubes on the flammability properties of acrylonitrile-butadiene-styrene composites, Polym. Int. 63 (2014) 1168–1173, doi:10.1002/pi.4653.

[67] B.K. Kandola, D. Deli, Flame-Retardant Thermoset Nanocomposites for Engineering Applications, 2014. 10.1016/B978-0-444-53808-6.00016-0.

[68] M. Rajaei, N.K. Kim, S. Bickerton, D. Bhattacharyya, A comparative study on effects of natural and synthesised nano-clays on the fire and mechanical properties of epoxy composites, Compos. Part B Eng. 165 (2019) 65–74, doi: 10.1016/j.compositesb.2018.11.089.

[69] A. Zubkiewicz, A. Szymczyk, S. Paszkiewicz, R. J ędrzejewski, E. Piesowicz, J. Siemiński, Ethylene vinyl acetate copolymer/halloysite nanotubes nanocomposites with enhanced mechanical and thermal properties, J. Appl. Polym. Sci. (2020) 1–12, doi:10.1002/app.49135.

[70] D.L. Francisco, L.B. Paiva, W. Aldeia, Advances in polyamide nanocomposites: A review, Polym. Compos. 40 (2019) 851–870, doi:10.1002/pc.24837.

[71] L.W. McKeen, Polyamides (Nylons), Film Prop. Plast. Elastomers. (2017) 187–227, doi:10.1016/b978-0-12-813292-0.00008-3.

[72] S.V. Levchik, E.D. Weil, Combustion and fire retardancy of aliphatic nylons, Polym. Int. 49 (2000) 1033–1073, doi:10.1002/1097-0126(200010)49:10⟨1033::AID-PI518⟨3.0.CO;2-I.

[73] J. Markarian, Flame retardants for polyamides - new developments and processing concerns, Plast. Addit. Compd. 7 (2005) 22–25, doi:10.1016/S1464-391X(05)00357-0.

[74] Q. Li, B. Li, S. Zhang, M. Lin, Investigation on effects of aluminum and magnesium hypophosphites on flame retardancy and thermal degradation of polyamide 6, J. Appl. Polym. Sci. 125 (2012) 1782–1789, doi:10.1002/app.35678.

[75] M. Boonkongkaew, K. Sirisinha, Halloysite nanotubes loaded with liquid organophosphate for enhanced flame retardancy and mechanical properties of polyamide 6, J. Mater. Sci. 53 (2018) 10181–10193, doi:10.1007/s10853-018-2351-z.

[76] L. Li, Z. Wu, S. Jiang, S. Zhang, S. Lu, W. Chen, B. Sun, M. Zhu, Effect of halloysite nanotubes on thermal and flame retardant properties of polyamide 6/melamine cyanurate composites, Polym. Compos. 36 (2015) 892–896, doi:10.1002/pc.23008.

[77] D. Kijowska, P. Jankowski, E. Wierzbicka, Halloysite modified by melamine cyanurate and its compositions based on PA6, Polimery/Polymers 64 (2019) 259–266, doi:10.14314/polimery.2019.4.3.

[78] H. Vahabi, R. Sonnier, A. Taguet, B. Otazaghine, M.R. Saeb, G. Beyer, Halloysite nanotubes (HNTs)/polymer nanocomposites: thermal degradation and flame retardancy, in: Clay Nanoparticles, Elsevier, 2020, pp. 67–93, doi:10.1016/B978-0-12-816783-0.00003-7.

[79] M. Sahnoune, A. Taguet, B. Otazaghine, M. Kaci, J.M. Lopez-Cuesta, Fire retardancy effect of phosphorus-modified halloysite on polyamide-11 nanocomposites, Polym. Eng. Sci. 59 (2018) 526–534, doi:10.1002/pen.24961.

[80] L.L. Li, S.H. Chen, W.J. Ma, Y.H. Cheng, Y.P. Tao, T.Z. Wu, W.P. Chen, Z. Zhou, M.F. Zhu, A novel reduced graphene oxide decorated with halloysite nanotubes (HNTs-d-rGO) hybrid composite and its flame-retardant application for polyamide 6, Express Polym. Lett. 8 (2014) 450–457, doi:10.3144/expresspolymlett.2014.48.

[81] G. Huang, J. Gao, X. Wang, H. Liang, C. Ge, How can graphene reduce the flammability of polymer nanocomposites? Mater. Lett. 66 (2012) 187–189, doi:10.1016/j.matlet.2011.08.063.

[82] B. Tawiah, B. Yu, B. Fei, Advances in flame retardant poly(lactic acid), Polymers (Basel) 10 (2018), doi:10.3390/polym10080876.

[83] N.A. Isitman, M. Dogan, E. Bayramli, C. Kaynak, The role of nanoparticle geometry in flame retardancy of polylactide nanocomposites containing aluminium phosphinate, Polym. Degrad. Stab. 97 (2012) 1285–1296, doi:10.1016/j.polymdegradstab.2012.05.028.

[84] H. Kaya, E. Özdemir, C. Kaynak, J. Hacaloglu, Effects of nanoparticles on thermal degradation of polylactide/aluminium diethylphosphinate composites, J. Anal. Appl. Pyrolysis. 118 (2016) 115–122, doi:10.1016/j.jaap.2016.01.005.

[85] Z. Li, D. Fernández Expósito, A. Jiménez González, D.Y. Wang, Natural halloysite nanotube based functionalized nanohybrid assembled via phosphorus-containing slow release method: A highly efficient way to impart flame retardancy to polylactide, Eur. Polym. J. 93 (2017) 458–470, doi:10.1016/j.eurpolymj.2017.06.021.

[86] A.A. Younis, Flammability properties of polypropylene containing montmorillonite and some of silicon compounds, Egypt. J. Pet. 26 (2017) 1–7, doi:10.1016/j.ejpe.2016.02.003.

[87] S. Shang, X. Ma, B. Yuan, G. Chen, Y. Sun, C. Huang, S. He, H. Dai, X. Chen, Modification of halloysite nanotubes with supramolecular self-assembly aggregates for reducing smoke release and fire hazard of polypropylene, Compos. Part B Eng. 177 (2019) 107371, doi:10.1016/j.compositesb.2019.107371.

[88] A. Jenifer, N. Rasana, K. Jayanarayanan, Synergistic effect of the inclusion of glass fibers and halloysite nanotubes on the static and dynamic mechanical, thermal and flame retardant properties of polypropylene, Mater. Res. Express. 5 (2018), doi:10.1088/2053-1591/aac67d.

[89] A. Subasinghe, R. Das, D. Bhattacharyya, Study of thermal, flammability and mechanical properties of intumescent flame retardant PP/kenaf nanocomposites, Int. J. Smart Nano Mater. 7 (2016) 202–220, doi:10.1080/19475411.2016.1239315.

[90] Z. Jia, Y. Luo, B. Guo, B. Yang, M. Du, D. Jia, Reinforcing and flame-retardant effects of halloysite nanotubes on LLDPE, Polym. - Plast. Technol. Eng. 48 (2009) 607–613, doi:10.1080/03602550902824440.

[91] L. Dumazert, D. Rasselet, B. Pang, B. Gallard, S. Kennouche, J.M. Lopez-Cuesta, Thermal stability and fire reaction of poly(butylene succinate) nanocomposites using natural clays and FR additives, Polym. Adv. Technol. 29 (2018) 69–83, doi:10.1002/pat.4090.

[92] Y. Wang, C. Liu, X. Shi, J. Liang, Z. Jia, G. Shi, Synergistic effect of halloysite nanotubes on flame resistance of intumescent flame retardant poly(butylene succinate) composites, Polym. Compos. 40 (2019) 202–209, doi:10.1002/pc.24629.

[93] S. Remanan, M. Sharma, P. Jayashree, J. Parameswaranpillai, T. Fabian, J. Shih, P. Shankarappa, B. Nuggehalli, S. Bose, Unique synergism in flame retardancy in ABS based composites through blending PVDF and halloysite nanotubes, Mater. Res. Express. 4 (2017), doi:10.1088/2053-1591/aa7617.

[94] S.M.D.M. Saheb, P. Tambe, M. Malathi, Influence of halloysite nanotubes and intumescent flame retardant on mechanical and thermal properties of 80/20 (Wt/wt) pp/ABS blend and their composites in the presence of dual compatibilizer, J, Thermoplast. Compos. Mater. 31 (2018) 202–222, doi:10.1177/0892705717697775.

[95] H.B. Chen, Y.Z. Wang, D.A. Schiraldi, Preparation and flammability of poly(vinyl alcohol) composite aerogels, ACS Appl. Mater. Interfaces. 6 (2014) 6790–6796, doi:10.1021/am500583x.

[96] G. George, M. Selvakumar, A. Mahendran, S. Anandhan, Structure-property relationship of halloysite nanotubes/ethylene-vinyl acetate-carbon monoxide terpolymer nanocomposites, J, Thermoplast. Compos. Mater. 30 (2017) 121–140, doi:10.1177/0892705715588802.

[97] B. Lecouvet, M. Sclavons, S. Bourbigot, C. Bailly, Thermal and flammability properties of polyethersulfone/halloysite nanocomposites prepared by melt compounding, Polym. Degrad. Stab. 98 (2013) 1993–2004, doi:10.1016/j.polymdegradstab.2013.07.013.

[98] P.S. Khobragade, D.P. Hansora, J.B. Naik, A. Chatterjee, Flame retarding performance of elastomeric nanocomposites: A review, Polym. Degrad. Stab. 130 (2016) 194–244, doi:10.1016/j.polymdegradstab.2016.06.001.

[99] S. Azarmgin, B. Kaffashi, S.M. Davachi, Investigating thermal stability and flame retardant properties of synthesized halloysite nanotubes (HNT)/Ethylene propylene diene monomer (EPDM) nanocomposites, Int. Polym. Process. 30 (2015) 29–37, doi:10.3139/217.2789.

[100] P. Rybiński, G. Janowska, Influence synergetic effect of halloysite nanotubes and halogen-free flame-retardants on properties nitrile rubber composites, Thermochim. Acta 557 (2013) 24–30, doi:10.1016/j.tca.2013.01.030.

[101] P. Rybiński, G. Janowska, Thermal stability and flammability of nanocomposites made of diene rubbers and modified halloysite nanotubes, J. Therm. Anal. Calorim. 113 (2013) 31–41, doi:10.1007/s10973-013-3035-1.

[102] P. Rybiński, A. Pająk, G. Janowska, M. Jóźwiak, Effect of hybrid filler (HNTs-phthalocyanine) on the thermal properties and flammability of diene rubber, J. Appl. Polym. Sci. 132 (2015) 1–20, doi:10.1002/app.42593.

[103] R. Anyszka, D.M. Bieliński, Z. Pędzich, P. Rybiński, M. Imiela, M. Siciński, M. Zarzecka-Napierala, T. Gozdek, P. Rutkowski, Thermal stability and flammability of styrene-butadiene rubber-based (SBR) ceramifiable composites, Materials (Basel) 9 (2016) 1–12, doi:10.3390/ma9070604.

[104] N. Saba, M. Jawaid, O.Y. Alothman, M.T. Paridah, A. Hassan, Recent advances in epoxy resin, natural fiber-reinforced epoxy composites and their applications, J. Reinf. Plast. Compos. 35 (2016) 447–470, doi:10.1177/0731684415618459.

[105] C. Martín, G. Lligadas, J.C. Ronda, M. Galià, V. Cádiz, Synthesis of novel boron-containing epoxy–novolac resins and properties of cured products, J. Polym. Sci. Part A Polym. Chem. 44 (2006) 6332–6344, doi:10.1002/pola.21726.

[106] X. Li, Y. Ou, Y. Shi, Combustion behavior and thermal degradation properties of epoxy resins with a curing agent containing a caged bicyclic phosphate, Polym. Degrad. Stab. 77 (2002) 383–390, doi:10.1016/S0141-3910(02)00075-7.

[107] M. Spontón, L.A. Mercado, J.C. Ronda, M. Galià, V. Cádiz, Preparation, thermal properties and flame retardancy of phosphorus- and silicon-containing epoxy resins, Polym. Degrad. Stab. 93 (2008) 2025–2031, doi:10.1016/j.polymdegradstab.2008.02.014.

[108] N. Saba, M. Jawaid, M.T. Paridah, O.Y. Al-othman, A review on flammability of epoxy polymer, cellulosic and non-cellulosic fiber reinforced epoxy composites, Polym. Adv. Technol. 27 (2016) 577–590, doi:10.1002/pat.3739.

[109] H. Vahabi, M.R. Saeb, K. Formela, J.M.L. Cuesta, Flame retardant epoxy/halloysite nanotubes nanocomposite coatings: Exploring low-concentration threshold for flammability compared to expandable graphite as superior fire retardant, Prog. Org. Coatings. 119 (2018) 8–14, doi:10.1016/j.porgcoat.2018.02.005.

[110] T. Zheng, X. Ni, Loading an organophosphorous flame retardant into halloysite nanotubes for modifying UV-curable epoxy resin, RSC Adv. 6 (2016) 57122–57130, doi:10.1039/c6ra08178a.

[111] Y. Dong, B. Lisco, H. Wu, J.H. Koo, M. Krifa, Flame retardancy and mechanical properties of ferrum ammonium phosphate-halloysite/epoxy polymer nanocomposites, J. Appl. Polym. Sci. 132 (2015) 1–12, doi:10.1002/app.41681.

[112] M. Zhang, Y. Cheng, Z. Li, X. Li, L. Yu, Z. Zhang, Biomass Chitosan-Induced Fe3O4 Functionalized Halloysite Nanotube Composites: Preparation, Characterization and Flame-Retardant Performance, Nano 14 (2019) 1–15, doi:10.1142/S1793292019501546.

[113] F. Wu, K. Pickett, A. Panchal, M. Liu, Y. Lvov, Superhydrophobic Polyurethane Foam Coated with Polysiloxane-Modified Clay Nanotubes for Efficient and Recyclable Oil Absorption, ACS Appl. Mater. Interfaces. 11 (2019) 25445–25456, doi:10.1021/acsami.9b08023.

[114] R.J. Smith, K.M. Holder, S. Ruiz, W. Hahn, Y. Song, Y.M. Lvov, J.C. Grunlan, Environmentally Benign Halloysite Nanotube Multilayer Assembly Significantly Reduces Polyurethane Flammability, Adv. Funct. Mater. 28 (2018) 1–8, doi:10.1002/adfm.201703289.